THESIS

THE AMYLOID BETA DIMER/TRIMER: A POTENT STIMULATOR OF NEURONAL AMYLOID BETA SECRETION AND COFILIN-ACTIN ROD FORMATION

Submitted by

Ian Marsden

Department of Biochemistry and Molecular Biology

In partial fulfillment of the requirements

For the Degree of Master of Science

Colorado State University

Fort Collins, Colorado

Fall 2010

Master's Committee:

Department Chair: Shing P. Ho

Advisor: James R. Bamburg

Santiago M. Di Pietro
Kathryn M. Partin

ABSTRACT

THE AMYLOID BETA DIMER/TRIMER: A POTENT STIMULATOR OF NEURONAL AMYLOID BETA SECRETION AND COFILIN-ACTIN ROD FORMATION

Amyloid beta (Aβ) peptides, a heterogeneous mixture of 39-43 amino acid peptides produced from β- and γ-secretase cleavage of the amyloid precursor protein (APP), are one of the causative agents of Alzheimer disease (AD). Although sensitive enzyme-linked immunosorbent assays (ELISAs) for specific rodent Aβ peptides and for total and specific human Aβ peptides have been commercially available, no commercial assay for total rodent Aβ was available when we began these studies. Such an assay is desirable to determine the effects of the human Aβ peptides on production of Aβ from cultured rodent neurons, the major model system used in AD research. Here we report an ELISA for total rodent Aβ and show that it can be used without interference from physiologically relevant concentrations of human Aβ. We then apply the assay to measure the production of Aβ in cultured dissociated rat cortical neurons and rat and mouse hippocampal organotypic slices in response to oxidative stress or treatment with human Aβ dimer/trimer (Aβd/t) obtained from culture medium of Chinese hamster ovary cell line 7PA2 expressing a mutant form of human

amyloid precursor protein. Neither of the treatments leads to accumulation of intracellular Aβ peptides. Peroxide increases Aβ secretion by about 2 fold, similar to results from previous reports that used an immunoprecipitation and western blot assay. Of greater significance is that physiologically relevant concentrations (250 pM) of human Aβd/t increase rodent Aβ secretion by >3 fold over 4 days, providing support for an Aβ-mediated feed-forward model of AD progression. The over two fold increase in rodent Aβ secreted in response to human Aβd/t was nearly identical between organotypic hippocampal slices of *TAU* knock-out mice and *TAU* knock-out mice expressing the human tau transgene, demonstrating that tau plays no role in the enhanced production of Aβ.

Previous studies showed oligomers of synthetic amyloid beta ($A\beta_{1-42}$) induced cofilin activation and formation of cofilin-actin rods in a neuronal subpopulation of rat hippocampus primarily localized within the dentate gyrus. Here we demonstrate that Aβd/t at ~250 pM is more potent in rod induction in both dissociated hippocampal neuronal cultures and organotypic slices than is 1 μM synthetic Aβ as typically prepared oligomers, about a 4000 fold difference. Treatment of the Aβd/t fraction with an Aβ-neutralizing antibody eliminates its rod inducing activity. Traditionally prepared synthetic Aβ oligomers contain SDS-stable trimers and tetramers, but are devoid of dimers. When synthetic human Aβ was incubated under conditions that generate a tyrosine oxidized dimer, the concentration that was required to induce rods decreased dramatically. The oxidized dimer had a maximum rod-inducing activity at ~2 nM (10 ng/mL),

suggesting it is the presence of the SDS-stable tyrosine oxidized Aβ dimer in a low-n state that is largely responsible for the potency of the secreted Aβd/t.

Aβd/t-induced rods are highly localized to the dentate gyrus and mossy fiber pathway and form more rapidly (significant over controls by 2 h compared to 8 h for those induced by synthetic Aβ-oligomers). Aβd/t-induced rods are reversible, disappearing by 24 h after washout. Cofilin dephosphorylation in response to Aβd/t is greatest within the hippocampal regions of rod formation. Overexpression of cofilin phosphatases slingshot and chronophin increase rod formation when expressed alone and exacerbate rod formation when coupled with Aβd/t treatment both in dissociated neurons and organotypic slice cultures. Overexpression of the cofilin kinase, LIM kinase 1, inhibits Aβd/t-induced rod formation. Together these data support a mechanism through which Aβd/t produces selective synaptic dysfunction affecting learning and memory at least in part via primary effects on cofilin regulation and rod formation in sensitive hippocampal regions.

TABLE OF CONTENTS

CHAPTER ONE

β-AMYLOID-INDUCED β-AMYLOID SECRETION: A FEED-FORWARD MODEL FOR ALZHEIMER DISEASE.

Preface and Acknowledgement

The work presented in this chapter has been submitted to Journal of Alzheimer Disease. The order and list of authors is as follows: Ian T. Marsden, Laurie S. Minamide, and James R. Bamburg. We would like to thank Dr. Dennis Selkoe, BWH, Harvard Medical School for the gift of 7PA2 cells and Drs. Chi Pak, O'Neil Wiggan, Barbara Bernstein and Ms. Alisa Shaw for valuable discussions. The authors gratefully acknowledge funding from the NIH National Institute of Neurological Disorders and Stroke (NS40371 to J.R.B.)

Abstract

Amyloid beta (Aβ) peptides, a heterogeneous mixture of 39-43 amino acid peptides produced from β- and γ-secretase cleavage of the amyloid precursor protein (APP), are one of the causative agents of Alzheimer disease (AD). Although sensitive enzyme-linked immunosorbent assays (ELISAs) for specific rodent Aβ peptides and for total and specific human Aβ peptides have been

commercially available, no commercial assay for total rodent Aβ was available when we began these studies. Such an assay is desirable to determine the effects of the human Aβ peptides on production of Aβ from cultured rodent neurons, the major model system used in AD research. Here we report an ELISA for total rodent Aβ and show that it can be used without interference from physiologically relevant concentrations of human Aβ. We then apply the assay to measure the production of Aβ in cultured dissociated rat cortical neurons and rat and mouse hippocampal organotypic slices in response to oxidative stress or treatment with human Aβ dimer/trimer (Aβd/t). Neither of the treatments leads to accumulation of intracellular Aβ peptides. Peroxide increases Aβ secretion by about 2 fold, similar to results from previous reports that used an immunoprecipitation and western blot assay. Of greater significance is that physiologically relevant concentrations (250 pM) of human Aβd/t increase rodent Aβ secretion by >3 fold over 4 days, providing support for an Aβ-mediated feed-forward model of AD progression. The over two fold increase in rodent Aβ secreted in response to human Aβd/t was identical between organotypic hippocampal slices of *TAU* knock-out mice and *TAU* knock-out mice expressing the human tau transgene, demonstrating that tau plays no role in the enhanced production of Aβ.

Introduction

Alzheimer disease is the major form of dementia that affects the aged with about a 50% probability of occurrence in every person living to age 85 and

beyond (Alzheimer's Association, 2010). The pathological hallmarks of the disease are extracellular amyloid plaques, composed primarily of the amyloid beta peptide, and hyperphosphorylated tau inclusions in the form of striated neuropil threads and neurofibrillary tangles (Bamburg & Bloom, 2009). Familial AD, representing 1% or less of AD cases, arises from mutations in genes affecting the production or clearance in the brain of the 38-43 amino acid amyloid beta (Aβ) peptides (Tanzi & Bertram, 2005), which are excised from the transmembrane amyloid precursor protein (APP) through the actions of β- and γ-secretases (Glenner & Wong, 1984; Price et al., 1995; Hardy & Selkoe, 2002; Mattson, 2004). However, Aβ peptides also accumulate in the other 99% of AD cases, called sporadic AD, although the mechanisms driving its production are unclear (Mattson, 2004; Tanzi & Bertram, 2005).

Different isoforms and different conformations or aggregation states of the Aβ peptides deliver different signals to neurons and have remarkably different neuronal and synapto-toxicities. The $A\beta_{1-42}$ peptides are more amyloidogenic than the $A\beta_{1-40}$ peptides, and are more correlated with AD and its progression (Finder & Glockshuber, 2007; Portelius et al., 2010). Fibrillar forms of the Aβ species are less toxic than the soluble oligomeric forms (Krafft & Klein, 2010). An oligomeric fraction, called Aβ-derived diffusible ligands (ADDLs), has effects on synapses at submicromolar concentrations (Krafft & Klein, 2010). However, an even more active form of Aβ with maximal activity at subnanomolar concentrations, is secreted from a cultured cell line (7PA2 cells) expressing a mutated form of human APP (Walsh et al., 2002). This material contains SDS-

stable human Aβ (HAβ) dimers and trimers (HAβd/t), which can be isolated by gel filtration; the isolated HAβd/t has a marked effect on synaptic function, both in cultured slices and when injected into rodent brain (Cleary et al., 2005; Townsend et al., 2006; Shankar et al., 2007; Freir et al., 2010). An SDS-stable HAβ dimer has been extracted from postmortem human AD brain and is also active at subnanomolar concentrations (Shankar et al. 2008). The presence of the SDS-stable HAβ dimer is strongly correlated with AD type dementia (McDonald et al., 2010). Excessive production of HAβ from APP occurs in familial AD due to mutations in APP and its processing enzymes or in proteins that normally clear the excess HAβ, but the causative factors leading to excess HAβ production in sporadic AD are much less understood. HAβ is known to inhibit axonal transport of mitochondria and vesicles containing neurotrophin receptors in mouse hippocampal neurons within 60 min of treatment (Vossel et al., 2010). The transport inhibition is dependent on the presence of the microtubule-binding and stabilizing protein tau. It has been proposed that stalled vesicles containing APP might be the sites for enhanced production of HAβ (Maloney et al., 2005), since up to 70% of the Aβ secreted from cells arises from β- and γ-secretase cleavage of APP within the lipid raft environment of endosomes (Koo & Squazzo, 1994; Ehehalt et al., 2003; Thomas et al., 2006; Cirrito et al., 2008). Although ELISAs have been available for quantifying individually either $A\beta_{1-40}$ or $A\beta_{1-42}$ from rodents or humans (Fukumoto et al., 1999; Gasparini et al., 2004; Covance BetaMark x-40 SIG-38950, x-42 SIG-38952), no single ELISA for total rodent Aβ (RAβ) was available when we began these studies. Here we report the

development of an ELISA for total RAβ using the sandwich method requiring two primary antibodies. The capture antibody is on the ELISA plate, and is specific for RAβ. The detection antibody binds to both RAβ and HAβ in solution and has a detection probe (HRP) attached. We then demonstrate that this assay can be used in the presence of physiologically relevant amounts of HAβd/t and apply the assay to cultures of rat cortical neurons and rat and mouse organotypic hippocampal slices treated with HAβd/t and with peroxide, another neuronal stress agent previously shown to increase Aβ secretion.

Materials and Methods

Reagents

Unless otherwise noted, all chemicals are reagent grade and were obtained from Sigma-Aldrich Co. (St. Louis, MO), and all tissue culture reagents were obtained from Life Technologies (Carlsbad, CA). Synthetic human amyloid beta ($HA\beta_{1-42}$) was obtained from AnaSpec, Inc. (San Jose, CA), and synthetic rodent amyloid beta ($RA\beta_{1-42}$ and $RA\beta_{1-40}$) was a gift from Covance (Princeton, NJ). The HAβ monomer (HAβm) and dimer/trimer (HAβd/t) fractions were prepared from the conditioned medium from Chinese hamster ovary (CHO) cells, clone 7PA2, expressing a mutant human APP (Walsh et al., 2002; a gift from Dennis Selkoe, Harvard Medical School), fractionated by size-exclusion chromatography as previously described (Townsend et al., 2007). Unless otherwise noted, it was used at the equivalent of 1x concentration (250 pM, the concentration of HAβd/t found in the conditioned medium). Medium from wild

type CHO cells was fractionated identically by size-exclusion, and fractions at the equivalent elution positions of HAβd/t were used as one control.

Dot-blot assay for quantifying Aβ in 7PA2 cell medium

HAβ was quantified in 7PA2 cell culture medium using dot blots with synthetic human β-amyloid peptide ($HA\beta_{1-42}$) as a standard as previously described (Davis et al., submitted). Briefly, samples were applied to nitrocellulose (0.1 μm), the membrane was boiled 10 min in PBS, and HAβ was detected with 6E10 antibody (overnight at 4^{o}C) followed by a goat-anti-mouse antibody conjugated to DyLight 680 (1:15,000 for 45 min; Thermo Scientific, Rockford, IL). Spots were imaged with a LI-COR Odyssey Infrared Imaging System, and intensities quantified using TotalLab software (Nonlinear Dynamics, Newcastle upon Tyne, UK).

Sandwich ELISA

Synthetic $RA\beta_{1-40}$ and $RA\beta_{1-42}$ were solubilized to 1 mg/mL in 0.1% ammonium hydroxide. Aliquots (10μL) were dried in a speed-vac and pellets were stored at -80°C. Costar 96-well white solid plates coated with 100 μL of either 2, 5, or 10 μg/mL of capture antibody, a rabbit polyclonal raised against amino acids 1-16 of RAβ, were provided by Covance (SIG-39153). The detection antibody is a horseradish peroxidase-conjugated mouse monoclonal, (SIG-39245; Covance) that is reactive to both HAβ and RAβ. Synthetic $RA\beta_{1-40}$ and $RA\beta_{1-42}$ pellets were solubilized in 10 μL of DMSO and diluted further with a

phosphate buffered saline containing Tween and BSA (PBSTB; Covance). Wells to be used on the assay plate were washed 1x with PBSTB and standards or samples (100 µL per well) were applied and plates incubated overnight at 4°C. Wells were washed 5x with 300 µL PBSTB. SuperSignal ELISA Pico Chemiluminescent Substrate (Thermo Scientific) was added at 300 µL to each well. Chemiluminescence was quantified by photon counting between 5 and 10 minutes using a Perkin-Elmer Victor V multi-mode microplate reader operating at room temperature with no filter.

Human Aβ interference in rodent Aβ ELISA:

$HA\beta_{1-42}$ (AnaSpec) was solubilized with 1,1,1,3,3,3-Hexafluoro-2-propanol to 1 mg/mL. Aliquots (10 µL) were allowed to air dry at room temperature and pellets were frozen at -80°C. Pellets were solubilized with 10 µL of DMSO, and diluted with Neurobasal containing B27 supplement to their desired concentration. In one set of experiments $RA\beta_{1-42}$ was maintained at 150 pg/mL and the amount of $HA\beta_{1-42}$ was varied from 10 pg/mL to 1 µg/mL. In a second set of experiments $HA\beta_{1-42}$ was maintained at 1.9 ng/mL (about the highest concentration of HAβd/t used in cell treatments) and RAβ was varied. Tubes containing mixed HAβ and RAβ were placed at 37°C for 72 hrs to mimic any co-oligomerization between human and rodent Aβ that might occur during the three days in which rodent cells are exposed to HAβ. Detection antibody at a final concentration of 1 µg/mL was added to the samples and after incubation for 30

min, samples were added to sandwich ELISA plates and processed as described for Sandwich ELISA.

DNA Assay

Calf Thymus DNA was solubilized with 100 mM Tris, 10 mM EDTA, pH 8.0 (TE buffer) and its final concentration determined spectrophotmetrically using an extinction coefficient of .02 $\mu g/mL^{-1} \cdot cm^{-1}$ at 260nm. Cells grown in Lab-Tek 8 well chamber slides were lysed with 200 µL of DNA lysis buffer (25 mM NaOH, 10 mM EDTA, pH 12.0), and wells were washed 2x with 300 µL of TE buffer which was added to the lysate. Standards and samples were diluted with TE buffer containing 1:10,000 SybrGreen I (Life Technologies, Carlsbad, CA). Lysates from the dissociated neuronal cell cultures were diluted 1:50 in TE buffer containing SybrGreen I. Organotypic mouse hippocampal slices were removed from the coverslip and lysed in 200 µL of DNA lysis buffer for 30 min at room temperature and 600 µL of TE buffer was added to lower the pH. Slice lysates were further diluted 1:200 in TE buffer with SybrGreen I. Samples and standards were added at 100 µL per well onto 96-well white solid plates (Costar, Corning Inc.). Fluorescence was quantified for 0.1 s per well on a Perkin-Elmer Victor V multi-mode microplate reader equipped with fluorescein filters.

To determine if all DNA was released from cells during lysis, slides were mounted with ProLong Gold Antifade reagent supplemented with 1:10,000 SybrGreen I to visualize any remaining dsDNA using a Nikon Diaphot equipped with a 20x (.75NA) air objective a fluorescein filter cube and a Photometrics

CoolSNAP cf CCD camera. Fluorescence intensity was measured across entire images using MetaMorph v7.03 (MDS Analytical Technologies, Toronto, Canada). Wells containing no cells were used as negative controls.

Neuronal cell culture

Animal studies were performed according to The National Research Council's guide for the care and use of laboratory animals using protocols approved by the Institutional Animal Care and Use Committee. E18 rat cortical and hippocampal neurons were obtained from timed-pregnant dams purchased from Harlan (Indianapolis, IN) and were prepared as previously described (Minamide et al., 2000). After counting, 300,000 cells were plated per well onto 8 well chamber slides (Lab-Tek, Thermo Scientific, Portsmouth, NH) that had been coated with poly-D-lysine. Neurons were cultured in 400 µL of Neurobasal medium supplemented with 1x B27, 2 mM GlutaMAX, and 100 µg/mL Penicillin/Streptomycin.

Mouse N2a neuroblastoma cells were obtained from ATCC and cultured in Dubelco's Modified Eagle Medium (D-MEM) with 4.5 g/L D-glucose, 2 mM L-glutamine, 110 mg/L sodium pyruvate, and 10% fetal bovine serum. Cells were plated at 5,000 cells per well onto 8 well chamber slides. One day after plating, cells were stressed with varying concentrations of hydrogen peroxide. After 3 days the medium was collected and diluted 1:10 with PBSTB and processed identically as that from cultures of dissociated neurons.

To determine the amount of internal RAβ within cortical neurons we cultured neurons identically as if media were to be assayed for RAβ content. After cells were stressed for 3 days we removed the media, and washed the cells with PBS. Cells were lysed in PBSTB containing 0.1% NP-40 for 5 min at room temperature and the lysate was processed identically to the medium using the RAβ ELISA.

Organotypic hippocampal slice cultures

Hippocampal slices (400 μm thick) were prepared from P6 Sprague Dawley rat pups (Stoppini et al., 1991) and cultured on membranes in 6 well dishes as previously described (Davis et al., 2009). Hippocampal slices (300 μm thick) on glass coverslips were prepared from P7 mouse pups (*TAU*$^{-/-}$ (B6.Cg-Mapt$^{tm1(EGFP)Klt}$, Jackson Labs, Bar Harbor, ME) and *TAU*$^{-/-}$ mice carrying the human tau transgene (B6.Cg- Mapt$^{tm1(EGFP)Klt}$ Tg(MAPT)8cPdav/J). Washed coverslips (12x22mm) were treated with 2% 3-aminopropyltriethoxysilane in acetone (10 sec dip), rinsed, air dried and UV sterilized. Chick plasma (4 μL) was spread into a 5 mm diameter circle near one end of the cover slip, two slices were placed side by side on the plasma and the slices were covered with 8 μL of fresh plasma/thrombin mixture (20 μL chick plasma (Cocalico Biologicals Inc., Reamstown, PA) and 6 μL thrombin (150 NIH units/ml in water; MP Biomedicals, Inc.). After the plasma clotted, the coverslip was inserted into a flat sided tube (Nunclon Delta Tubes, Nalge Nunc, Rochester, NY) and 600 μL slice culture medium added. Tubes were placed at a 5^{o} angle in a roller incubator (10

revolutions per hour) at 35^{o}C. The original slice medium (per 205 mL: 50 mL horse serum, 50 mL Hanks BSS, 4 mL 25% glucose, 100 mL minimum essential medium containing glutamax (250 µL/100 mL), HEPES (4.76g/ L) and Pen/Strep (1 mL)) was replaced on day 2 with Neurobasal A medium containing (per 50 mL): 48 mL Neurobasal A, 180 µL 25% glucose, 625 µL Glutamax 1, 1 mL B27 supplements and 250 µL Pen/Strep. The Neurobasal A medium was replaced every 2-3 days. Slices were allowed to recover for at least 1 week after dissection before treatment.

Statistics

All experiments were performed a minimum of two times with at least triplicate samples for every point but only a single experiment is shown. Error bars on each plot are standard deviations across at least 3 samples, and p values were determined from paired two-tail t tests.

Results

Development of an ELISA for total rodent Aβ

Several ELISAs have been reported that measure a variety of Aβ species or conformations including assays for RA$\beta_{1\text{-}40}$ or RA$\beta_{1\text{-}42}$ (Fukumoto et al., 1999; Walsh et al., 2000; Stenh et al., 2005; Xia et al., 2009). However, no commercial ELISA was available for measuring total RAβ. Such an assay could be used to quantify the effects of various stress agents on Aβ secretion from cultured neurons with less effort and expense than having to quantify each species

independently. Covance, a company that manufactured ELISA plates for assaying either RAβ_{1-40} or RA$\beta_{1-42,}$ agreed to supply us with plates and reagents to optimize a total RAβ ELISA. We developed a sandwich ELISA in which an antibody specific to total RAβ is bound to the plate (capture antibody) and a horseradish peroxidase (HRP) conjugated detection antibody, directed against an epitope well separated from the capture antibody, is preincubated with the sample. To determine the optimal concentration of capture antibody that allowed for maximal binding of RAβ to the plate, we coated plates with varying concentrations (2, 5, 10 μg/mL) of capture antibody. Synthetic RAβ_{1-40} and RAβ_{1-42} were diluted (0-600 pg/mL), the HRP-conjugated detection antibody (1.6 μg/mL) was added and after 10 min the samples were placed in wells of the 96 well plate. Plates coated with 5 or 10 μg/mL capture antibody gave identical curves that were linear between 10-600 pg/mL Aβ and both RAβ_{1-40} and RAβ_{1-42} were recognized with equal affinity (Figure 1.1). The plate coated with 2 μg/mL of capture antibody became saturated above 400 μg/mL using either Aβ species (data not shown). Thus, all reported assays were performed on plates coated with 5 or 10 μg/mL capture antibody.

Determining the maximum level of HAβ that does not interfere in RAβ ELISA

Rodent and human Aβ peptides differ in sequence in only three residues (Arg5, Tyr10, and His13 in HAβ is replaced by Gly5, Phe10, and Arg13 in RAβ) that are all within the epitope recognized by the capture antibody. By inference this means that the epitope recognized by the detection antibody is subject to

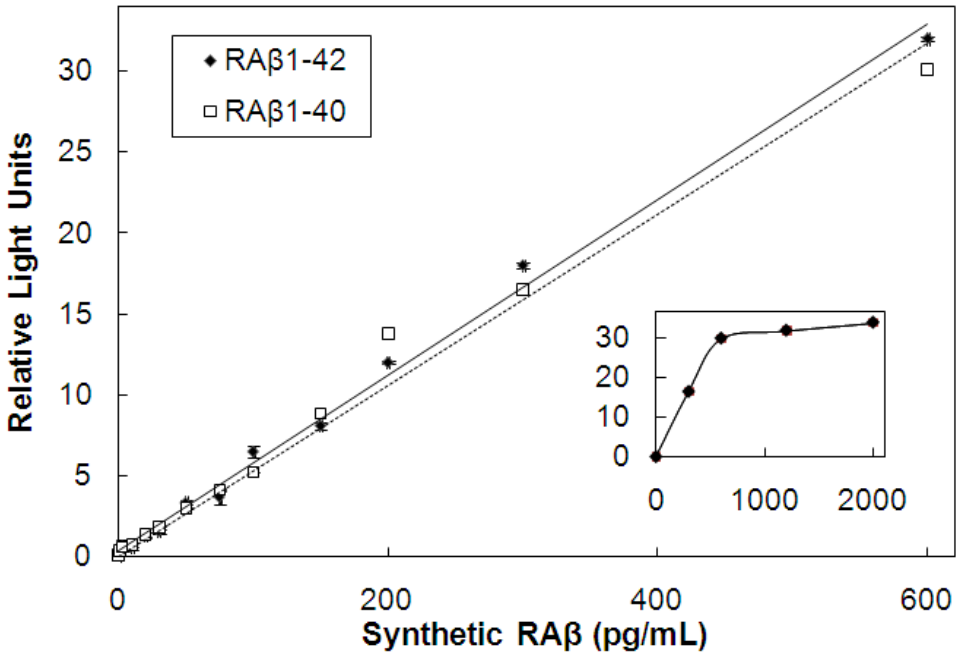

Figure 1.1. RAβ ELISA standard curves comparing $RA\beta_{1\text{-}40}$ and $RA\beta_{1\text{-}42}$. There is no significant difference between the two RAβ species in this assay. The assay is linear between 10 pg/mL and 600 pg/mL. Points are triplicate samples; error bars = standard deviation. Inset: the assay plateaus at RAβ concentrations above 600 ng/mL

interference by Aβ from non-rodent species. To be able to utilize the RAβ ELISA in the presence of HAβ, the maximum level of HAβ that could be tolerated in the assay needed to be determined. A constant level (150 pg/mL) of $RA\beta_{1-42}$ was maintained in the assay while $HA\beta_{1-42}$ was added from 10 pg/mL to 1 μg/mL (Figure 1.2A). $HA\beta_{1-42}$ at 5 ng/mL or less had no effect on the ability of the ELISA to correctly quantify the RAβ. The increased signal obtained at higher concentrations of HAβ could arise either from some weak affinity of the capture antibody for the HAβ or from co-oligomerization between RAβ and HAβ that might occur at higher Aβ concentrations (Fung et al., 2004; Jankowsky et al., 2007).

We also performed the RAβ ELISA using a constant amount of HAβ (1.9 ng/mL, approximately the maximum concentration in the HAβd/t fraction) with increasing concentrations of RAβ (from 10 pg/mL to 1μg/mL). At concentrations of RAβ below 600 pg/mL, the presence of the HAβ had no effect on the standard curve, demonstrating the ELISA is specific for RAβ within its linear region (Figure 1.2B).

Measurement of secreted RAβ from a rodent cell line

It was previously reported that peroxide induced secretion of Aβ from human neuroblastoma SH-SY5Y cells through JNK-dependent activation of γ-secretase (Shen et al., 2008). Therefore, we first utilized a mouse neuroblastoma cell line (N2a) to apply the RAβ ELISA. Mouse N2a cells were cultured in 8 well chamber slides and were stressed using varying levels of

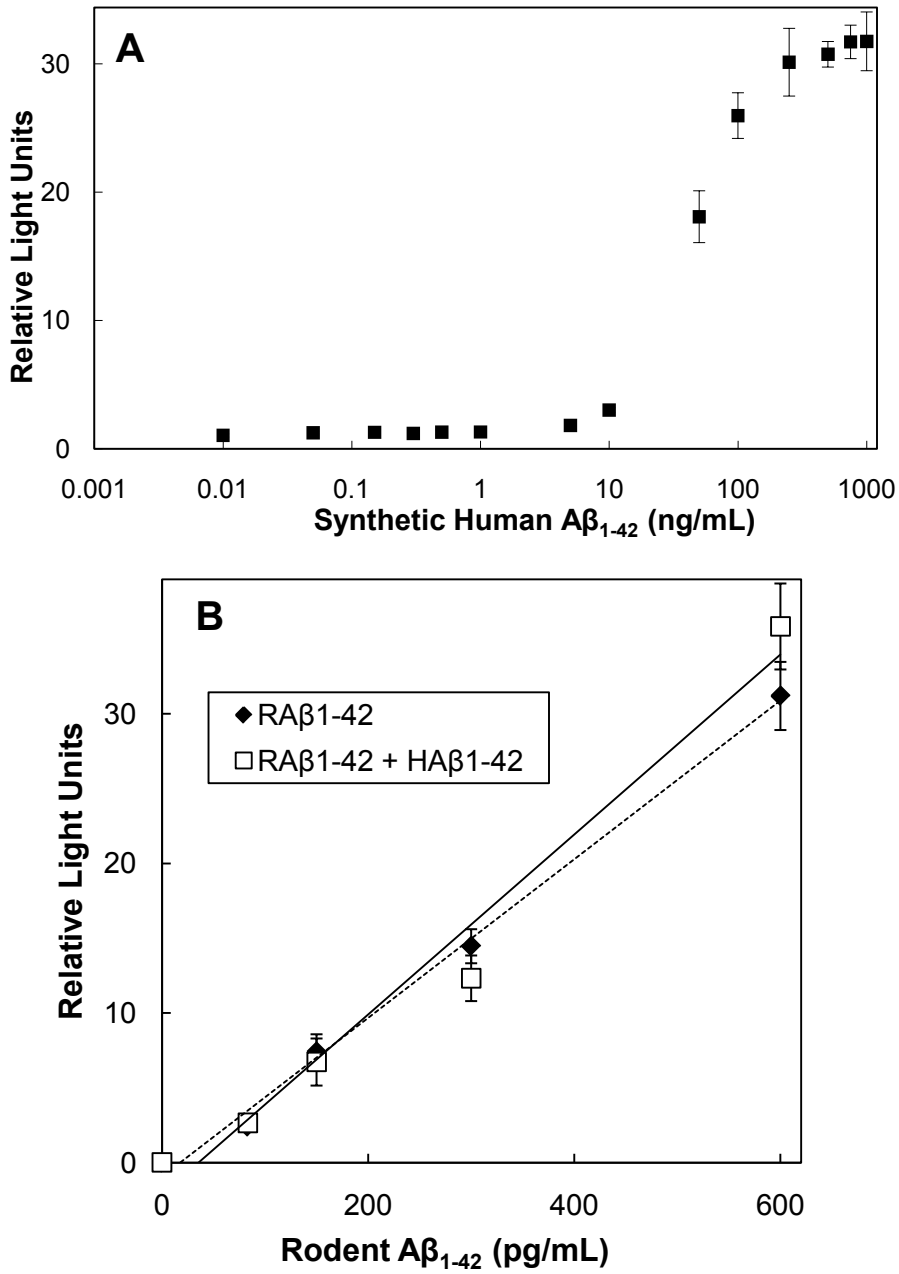

Figure 1.2. Effects of HAβ on the RAβ ELISA. (A) Effects of variable amounts of $HA\beta_{1-42}$ on the ability of the ELISA to detect a fixed amount (150 pg/ml) of $RA\beta_{1-42}$. Samples were incubated at 37°C to allow possible co-oligomerization to occur before the addition of detection antibody. Points are averages of triplicate samples; error bars = standard deviation (less than size of symbol for concentrations below 10 ng/mL). (B) Effects of a fixed amount of $HA\beta_{1-42}$ (1.9 ng/ml) on the RAβ ELISA standard curve. Samples of each concentration were incubated at 37°C for 3 days before assay to mimic the incubation conditions for secreted RAβ in the presence of the HAβd/t. Points are averages of triplicate samples; error bars = standard deviation.

hydrogen peroxide (0.5 mM to 10 mM) for 3 days. Medium was harvested and assayed for RAβ in triplicate wells. There was a significant increase ($p \leq 0.05$) in secreted RAβ levels for peroxide concentrations above 0.5 mM when compared to untreated controls with a maximum of over 5 fold obtained when treating with 2 mM peroxide (Figure 1.3). However, it was obvious from phase microscopy observation of the wells that significant cell loss occurred, especially at peroxide concentrations above 2 mM.

To normalize Aβ secretion to cell number we applied an assay to measure DNA levels in cultured cells, using the DNA binding dye SybrGreen I, which does not react with nucleotides, RNA, single-stranded nucleic acids, and proteins, as may occur with other DNA binding dyes (Kricka, 2002). DNA standard curves generated from calf thymus DNA were linear between 1-300 ng/mL (Figure 1.4). To normalize the Aβ secreted by the peroxide treated N2a cells to cell number, medium was removed from each well and analyzed for total RAβ and the remaining cells were lysed, the lysates diluted, and the DNA quantified. When normalized for secreted RAβ on a per cell basis, secretion of RAβ increased with increasing peroxide up to a maximum at 2 mM (Figure 1.3).

Application of the RAβ ELISA to primary neurons

Primary E18 rat cortical neurons were cultured in 8 well chamber slides for 3 days, and were left untreated or treated with varying concentrations of peroxide. Three days later culture medium was removed and assayed for RAβ. Neurons were washed once with PBS, lysed, and the lysates were used to

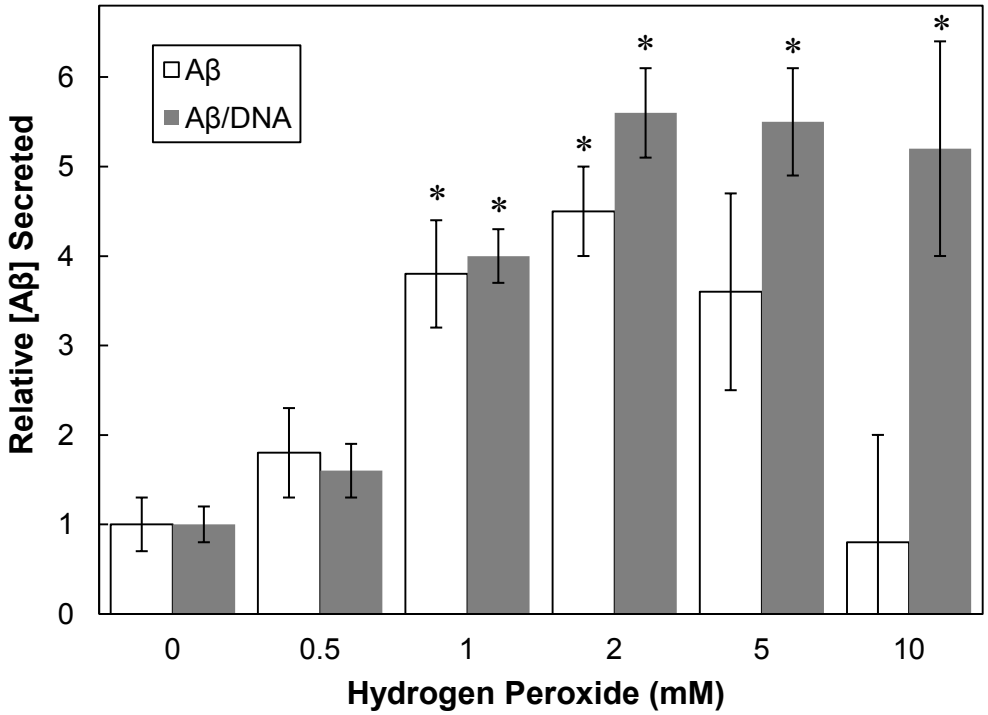

Figure 1.3. N2a cells were treated with different concentrations of hydrogen peroxide and the total RAβ secreted was determined after 3 days and normalized to levels secreted from untreated cells. An apparent decline in secreted Aβ occurred at peroxide concentrations above 2 mM. However, after correcting for cell loss by normalizing secreted Aβ to DNA in each well, the production of Aβ reached a plateau at or above 2 mM peroxide. * values of $p \leq 0.05$ compared to untreated samples.

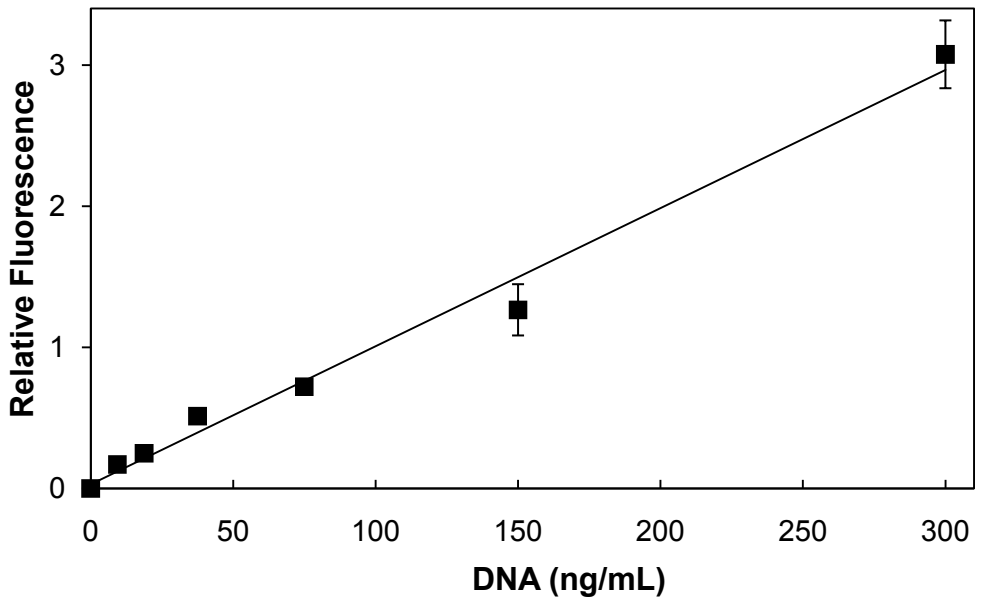

Figure 1.4. Standard curves for DNA using calf thymus DNA dissolved in TE as the standard. Standards and cell lysates are diluted with TE and SybrGreen I and then assayed using a microtiterplate reader operating in the fluorescence mode. The assay is linear between 1 ng to 300 ng/mL of DNA, but linearity can be expanded by adjusting the intensity of fluorescence or exposure time. Points are triplicate samples; error bars = standard deviation.

quantify either DNA (using the DNA Lysis Buffer) or the internal pool of RAβ using PBSTB w/ 0.1% NP-40).

Untreated neurons secreted 63 ± 5 pg (n=3) of Aβ per well equating to 157.0 pg/mL over the course of three days. By normalizing the concentration of Aβ to the DNA content of the well (1.72 ± .09 µg), we calculate that there are 0.036 pg Aβ/ng of DNA (Figure 1.5A). To determine the number of molecules secreted by each cell one can assume that there is 6.5 pg of DNA/cell (Ausubel et al., 1994); therefore, over a three day period, each cell secretes 220 ag of RAβ (or ~29,000 molecules), which equals about 6-7 RAβ peptides per minute/neuron under non-stress growth conditions.

Cortical neurons were stressed for 3 days with various concentrations (1 µM – 10 mM) of hydrogen peroxide, media were collected and RAβ contents were measured and normalized to DNA (Figure 1.5A). Concentrations of peroxide over 2 mM resulted in increasing cell death, observed by a decline in overall DNA content (data not shown). When compared to untreated neurons there was a significant ($p \leq 0.05$) increase in RAβ secreted only at or above peroxide concentrations of 100 µM, with a maximal secretion observed at 2 mM peroxide, resulting in a 2.4 ± 0.2 fold increase over untreated neurons (Figure 1.5A). This fold increase is similar to the increase (2.4 ± 0.6 fold over controls) observed in chick tectal neurons exposed to 10-20 µM peroxide for 20 h (Goldsbury et al., 2008). It is important to note that we elected to keep the B27 supplements in the neuronal culture medium because the supplements contain factors in addition to anti-oxidants (including catalase) that help keep the cells

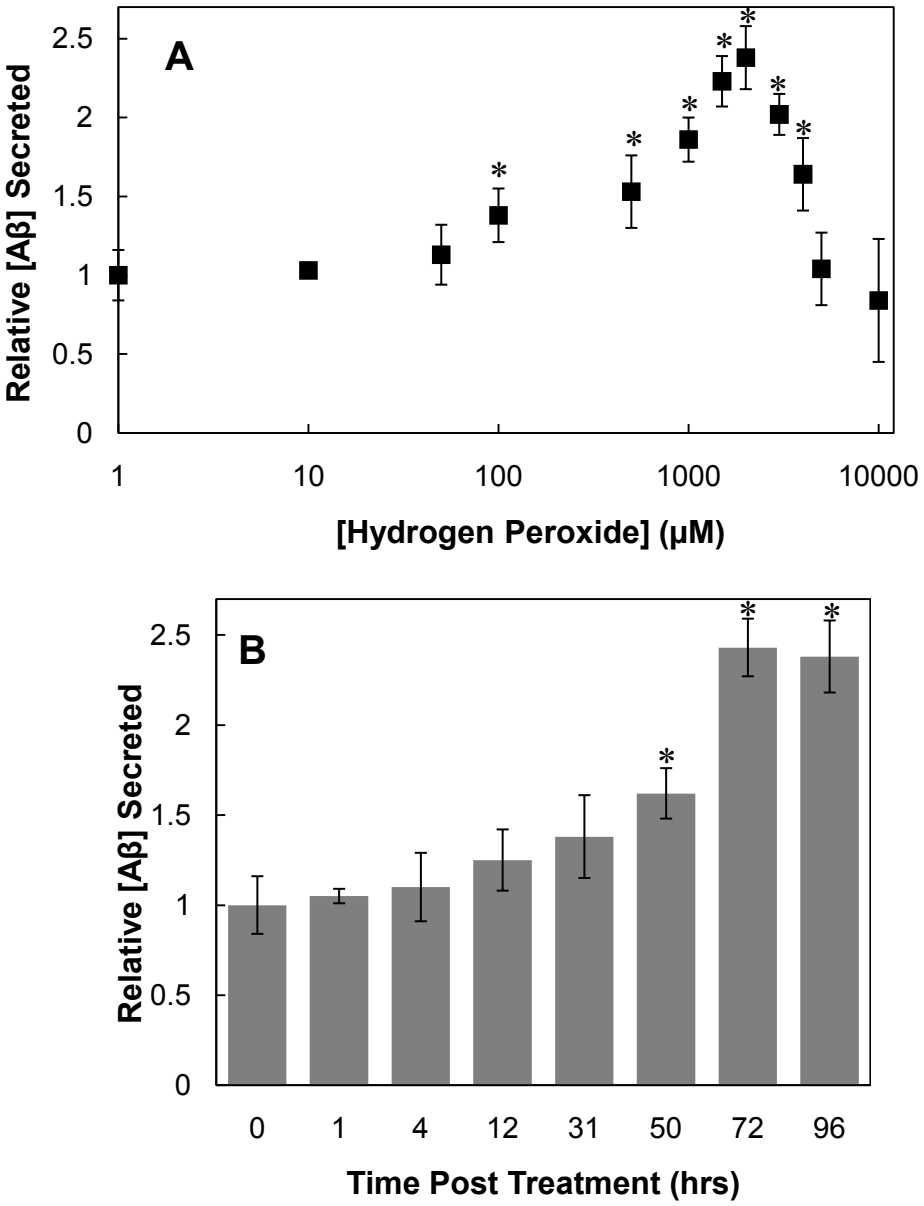

Figure 1.5. Effects of peroxide on secretion of RAβ from primary cortical neurons. (A) Normalized dose-response of RAβ secretion to hydrogen peroxide in rat E18 cortical neurons cultured in 8 well chamber slides. After 3 days of exposure, medium was removed from each well and cells were lysed with DNA lysis buffer. Medium was analyzed to determine the concentration of secreted RAβ and the cell lysate was analyzed to determine the DNA content. Values were normalized to untreated wells. Points are averages of triplicate samples; error bars = standard deviation, * values with $p \leq 0.05$ compared to untreated. RAβ secretion peaks with the addition of 2 mM peroxide. (B) Time course of RAβ secreted from rat E18 cortical neurons in response to 2 mM peroxide treatment. Medium was removed for RAβ assay and cells were lysed for DNA measurement at the times indicated. Points are averages of triplicate samples, error bars = standard deviation, * values with $p \leq 0.05$ compared to 0 time.

viable over the three day culture period. Thus, much higher concentrations of peroxide were required in these experiments than were needed to induce secretion in chick tectal neurons.

An increase in the internal pool of RAβ has been reported in neurons responding to certain types of stress (Hasegawa et al., 2005) and has been associated with synaptic dysfunction in mouse models of AD (Oddo et al., 2003; Casas et al., 2004). Thus, we quantified the internal pool of RAβ in lysed neurons untreated or treated with peroxide. The internal RAβ was not significantly different between untreated and peroxide-treated neurons. Untreated neurons had 4.3 $\pm$ 0.6 pg of RAβ per ng DNA and 2 mM peroxide-treated neurons contained 4.9 $\pm$ 0.8 pg of RAβ per ng DNA.

We next determined the time course of RAβ production in cortical neurons stressed with 2 mM peroxide. Neurons were plated identically as above and stressed with peroxide, with medium being collected after peroxide treatment at 24 h intervals up to 4 days. Although increased secretion was observed as early as 12 h after treatment, the increase was not statistically significant ($p \leq 0.05$) until 50 hrs, with maximal secretion obtained at 72 hrs (Figure 1.5B).

Because dissociated neurons might behave differently from neurons that maintain their connections with glia and other neurons, we also determined how peroxide affected the secretion of RAβ from rat hippocampal organotypic slices. Slices that had been grown on membranes for > 1 week (to allow recovery from the stress of preparation) were treated with 2 mM peroxide and after three days the culture medium was harvested and assayed for RAβ. The slices were lysed

for DNA quantification. When RAβ levels are compared to untreated slices on a per slice basis there is a 2.1 ± 0.3 fold increase; however when normalized to DNA, the fold increase is 1.5 ± 0.3, which is still significant but less than from the 2.4 fold increase observed for dissociated cortical neurons (Figure 1.6). Each untreated slice secretes 85 ± 8 pg (n=3) of RAβ over the course of 3 days.

HAβ dimer/trimer induces secretion of RAβ

Although synthetic HAβ peptides are usually used at concentrations well above 10 nM (45 ng/mL) to obtain any physiological or morphological changes in neurons, the secreted form of HAβ containing SDS-stable dimers and trimers (HAβd/t) (Walsh et al., 2002) and HAβ dimers extracted from postmortem AD brain (Shankar et al., 2008) are active at concentrations in the pM range (Freir et al., 2010), well below the levels of HAβ that interfere in our rodent ELISA. Thus we can for the first time directly assay the effects of physiologically relevant amounts of HAβ on RAβ secretion.

The conditioned medium from 7PA2 and wild type CHO cells was fractionated as previously described (Townsend et al., 2007). Fractions that contained primarily monomer (Aβm) and Aβd/t were obtained (Figure 1.7). The amount of HAβ in each fraction was quantified using a dot blot assay, because after adherence of the HAβ species the membrane could be boiled to expose the epitopes for detection. This step is essential for quantification of HAβ because oligomers are inefficiently measured by ELISA (Stenh et al., 2005), but it is not required for the RAβ assays, including the ELISA, because RAβ does not

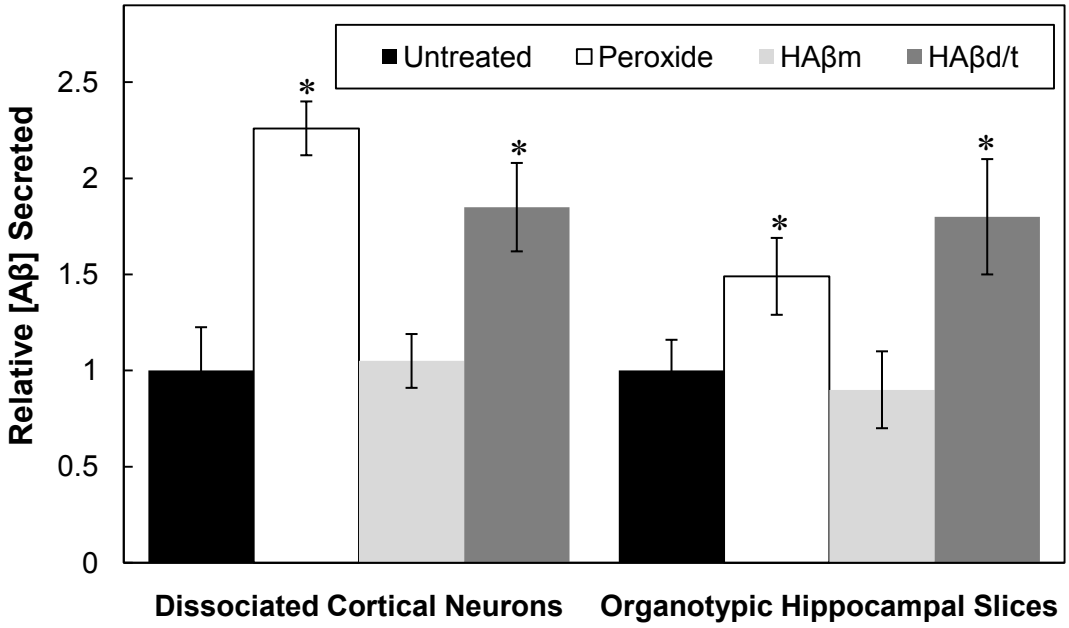

Figure 1.6. Comparison of effects of hydrogen peroxide (2 mM), HAβm, and HAβd/t on RAβ secretion from dissociated cortical neurons and organotypic hippocampal slices. Media from both neuronal and slice cultures were harvested 3 days after peroxide addition, RAβ levels were analyzed by ELISA, normalized to DNA, and expressed relative to untreated wells. Bars are average values from triplicate samples; error bars = standard deviation; * values with $p \leq 0.05$ compared to their untreated control.

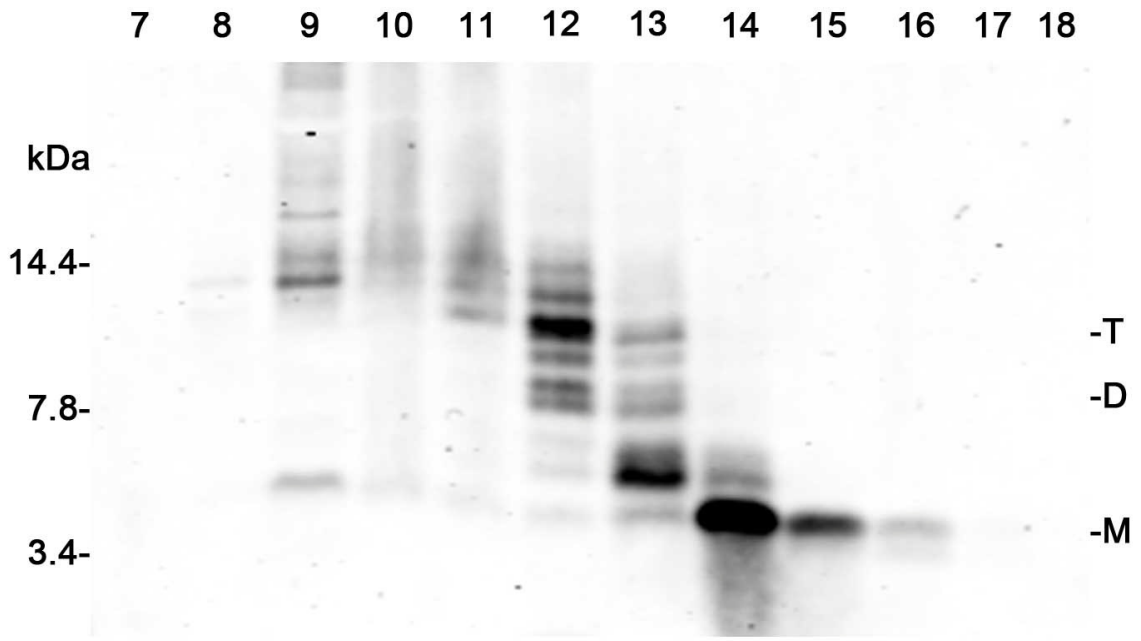

Figure 1.7. Western blot showing fractions of the HAβm and HABd/t from 10x concentrated culture medium of 7PA2 cells. The elution positions of monomer, dimer and trimer are shown. A total of 800 µl was removed from each fraction and stored at –80°C. The remaining 200 µl was lyophilized, resuspended in 2x sample buffer, and electrophoresed on a 10–20% Tris-Tricine gel. Proteins were transferred onto 0.1 µm nitrocellulose and detected, after boiling the blot for 10 min, by Western blotting for Aβ with 6E10 mouse monoclonal antibody and DyLight secondary antibodies detected with a Li-Cor Odyssey Infrared Imaging System. Fractions enriched in monomer (fractions 14-16) or dimer/trimer (fractions 12 and 13) were pooled separately, lyophilized, and stored at –80°C. They were used at the equivalent of 1x to treat cells. The amounts of HAβ in each fraction were determined by a dot blot assay described elsewhere (Chapter 2).

oligomerize at its secreted concentrations. The HAβm and HAβd/t fractions, as well as their respective controls (equivalent fractions from gel filtration of wt CHO cell medium), were added to 3 day old cultures of rat cortical neurons. Secreted rodent Aβ was quantified at 0, 24, 48, 72 and 96 h and normalized to the amount of DNA in each sample (Figure 1.8). The presence of HAβ did not interfere in the RAβ ELISA, as previously shown in Figure 1B, and confirmed here by the lack of change between untreated and HAβ-treated groups at time zero (Figure 1.8). Neurons treated with the HAβd/t, but not monomer or fractions from control CHO cell medium, induced secretion of RAβ to more than a 3-fold increase over controls by 4 days. Because of the possible co-oligomerization between the HAβd/t and the RAβ that could alter the assay results, we boiled some of the samples to enhance epitope exposure before performing the RAβ ELISA, but no differences between the boiled and unboiled samples were detected (data not shown). By 96 h the amount of RAβ was nearly identical to the amount of human Aβd/t added, so if co-oligomerization had occurred we should have observed an enhanced signal after boiling.

The effects of HAβm and HAβd/t on the secretion of RAβ from rat hippocampal organotypic slices was also determined. Slices were grown essentially as described in the peroxide experiments, and were treated with HAβm or HAβd/t and harvested 3 days after insult (Figure 1.6). When RAβ levels are compared to untreated slices on a per slice basis, there is no change in RAβ with HAβm treatment (0.9 ± 0.2 fold change), however HAβd/t treatment caused a significant ($p \leq 0.05$) 1.8 ± 0.2 fold increase in secreted RAβ. When

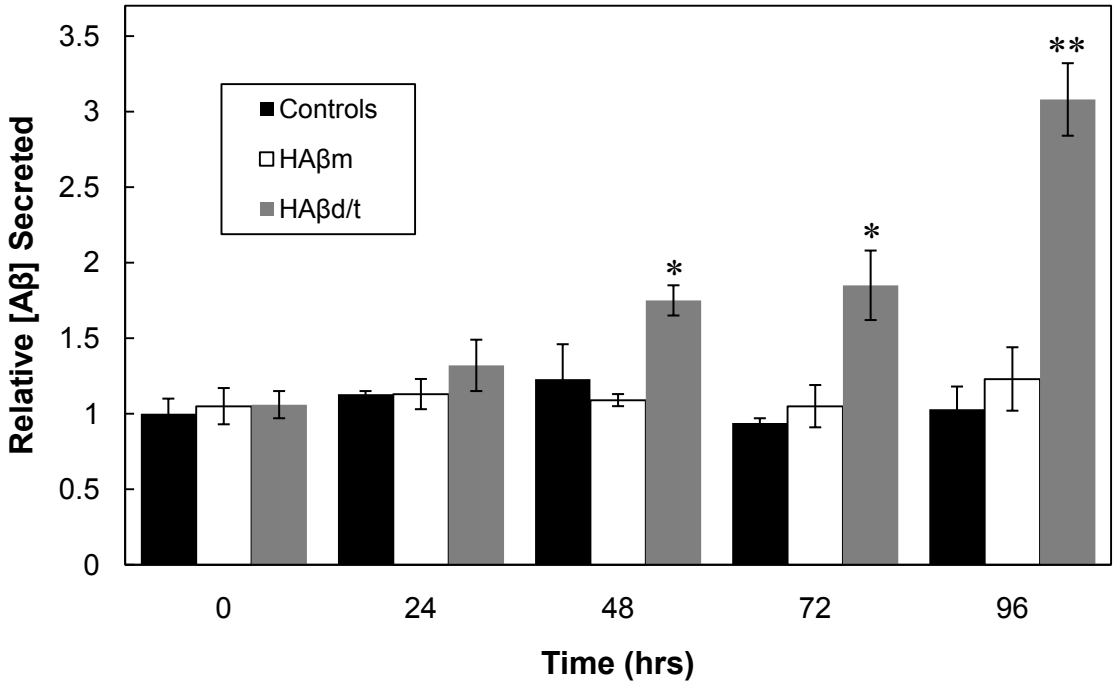

Figure 1.8. Time course of RAβ production from rat cortical neurons, untreated or treated with HAβm or HAβd/t fractionated from 7PA2 culture medium. Rat cortical neurons grown 3 days were left untreated or were treated with gel filtered fractions containing HAβm (3.6 ng/mL), HAβd/t (1.1 ng/mL) or equivalent volumes of the same fractions from wild type CHO cell culture medium (controls). Medium was removed at 0, 24, 48, 72, and 96 hrs after HAβ addition, and analyzed for RAβ. Cells were lysed and DNA measured for normalization. Values were then expressed relative to the untreated samples at time=0. All controls using fractionated medium from wild type CHO cells were not significantly different from the untreated controls of the same time point. Bars are average values from triplicate samples; error bars = standard deviation; * values with $p \leq 0.05$, or ** $p \leq 0.05$, compared to their untreated control.

organotypic hippocampal slices are compared to cortical neurons treated with HAβd/t there is a similar fold increase in RAβ secretion with both types of neurons.

There was no significant change in the amount of RAβ in the intracellular pool measured in lysates of cells treated with HAβd/t. Normalized per ng of DNA, untreated neurons had 5.1 $\pm$ 0.4 pg of RAβ, cells treated with HAβm had 4.8 $\pm$ 0.3 pg, and cells treated with HAβd/t had 5.4 $\pm$ 0.5 pg of rodent Aβ. These values were similar to the intracellular RAβ amounts reported above for the control and peroxide treated neurons (4.3 to 4.9 ± 0.8 pg).

To determine if the effects of HAβd/t on RAβ secretion are dependent on the microtubule protein tau, organotypic hippocampal slices from transgenic mice with either tau null *(TAU-/-*) or *TAU-/-* carrying a human tau transgene were used. These slices were cultured in pairs on glass coverslips in 0.6 mL of medium, which minimized the amount of HAβd/t required. Slices were stressed with 2 mM peroxide, HAβm (at 3.6 ng/ml), or HAβd/t (1.1 ng/ml) after slices had stabilized. After 3 days of treatment RAβ levels were quantified and normalized to DNA content (Figure 1.9). Both tau null slices and slices expressing the transgenic human tau showed a nearly identical increase in levels of RAβ when stressed with peroxide (1.6 ± 0.2 and 1.5 ± 0.2, respectively). Slices treated with HAβm showed no change in RAβ levels when compared with untreated slices. RAβ secreted from slices treated with HAβd/t increased 2.1 $\pm$ 0.3 fold (tau null) and a 2.3 $\pm$ 0.3 fold (transgenic human tau). Taken together, these results suggest that Aβ secretion is not dependent on tau.

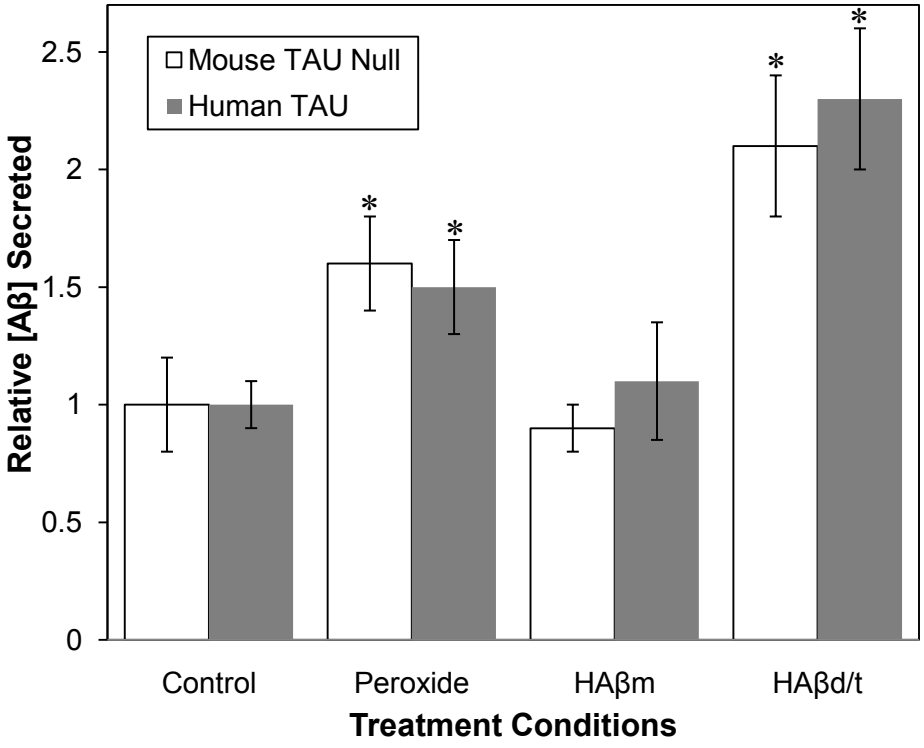

Figure 1.9. The presence or absence of tau has no effect on RAβ secretion induced by either peroxide or HAβd/t. Triplicate roller tubes containing two organotypic hippocampal slices from mice of genotype mouse *TAU*$^{-/-}$ or mouse *TAU*$^{-/-}$ with a human tau transgene were cultured for 10 or more days and then treated with 2 mM peroxide, HAβm (3.6 ng/mL) or HAβd/t (1.1 ng/mL). After 3 days, medium was harvested for measurement of secreted RAβ and tissue was lysed to measure DNA for normalization. Bars are averages of triplicate samples, error bars = standard deviations; * values with p≤0.05 compared with mouse *TAU*$^{-/-}$ control.

Discussion

Transgenic mice expressing human mutant APP are commonly used for AD research, but these animals also express endogenous mouse APP, which limits their usefulness when trying to measure effects on APP processing and Aβ release since quantifying mixed species of Aβ is more complex. In addition, HAβ peptides oligomerize and oligomers are not efficiently measured by a typical ELISA (Stenh et al., 2005), unless samples are denatured by boiling or treated with denaturants, both of which may decrease the accuracy of their determination. Furthermore, a goal of our work is to apply an ELISA for measuring RAβ secreted in response to treatment of cells with HAβ oligomers, something that is not feasible to do in cells secreting HAβ. Thus we developed an assay for total RAβ which can be used in the presence of physiologically relevant concentrations of HAβ oligomers. The advantage of the use of rodent neurons from non-transgenic animals is several fold: (1) they are easier to obtain and maintain than transgenic animals (Castrop, 2010); (2) rodent neurons (hippocampal and cortical) are the standard model system for studying the behavioral effects of HAβ treatment, both electrophysiologically and morphologically (Wang et al., 2004; Cleary et al., 2004; Shankar et al., 2007; Shankar et al., 2008; Freir et al., 2010); (3) the RAβ they produce does not oligomerize eliminating any need for boiling or denaturing higher order complexes before analysis (Atwood et al., 2004; Marksteiner & Humpel, 2008); (4) both rat and mouse Aβ peptides have the identical sequences and either species can be used for these assays (Johnstone et al., 1991).

Chick neurons produce Aβ with sequence, isoform patterns, and oligomerization patterns identical to HAβ (Esselmann et al., 2004; Carrodeguas et al., 2005), making them a useful system for some studies, but not for experiments in which treatment with HAβ is desired. Previously it was shown that 10-20 μM peroxide treatment causes a 2.4 fold increase in secreted Aβ after 20 hours in chick tectal neurons using an immunoprecipitation and Western blotting assay (Goldsbury et al., 2008). Only monomeric Aβ was quantified because it was the only species to show up on the western blots, perhaps because SDS-stable oligomers would not be visualized without boiling the membrane. In our assays, which were performed in the presence of the B27 supplement, we obtained no effect on RAβ production until we exceeded 100 μM hydrogen peroxide, demonstrating the protective effect of the B27 antioxidants and explaining why we required using much higher levels of peroxide than in previous studies in which neurons were maintained for shorter time periods (less than 24 h) (Goldsbury et al., 2008).

Conventional approaches to studying Aβ secretion in cultured neurons focus on overexpressing human APP, and measuring HAβ secreted into the extracellular environment (Busciglio et al., 1993; Suzuki et al., 1994). Here we show that this method might cause artificially high levels of secreted HAβ, simply due to the fact that there is a positive feedback loop where HAβd/t secreted can cause a further increase in HAβ secretion. Furthermore when using an ELISA to quantify the amount of HAβ secreted, low values are often observed because antibodies recognize different oligomers with varying affinities (Stenh et al.,

2005); however RAβ does not oligomerize making it easier to get accurate values on its secreted level. When using the ELISA to look at HAβ-induced RAβ secretion it is necessary to use the highly active naturally secreted Aβ dimer containing fractions (either from AD brain or 7PA2 conditioned medium) since synthetic HAβ is required at concentrations well above those that interfere with the RAβ ELISA.

HAβm does not show any synaptic detrimental effects and it has a role in neuroprotection, perhaps acting as a scavenger for metal induced oxidative stress (Zou et al., 2002). Here we show that HAβm does not cause an increase in RAβ secretion providing additional support that HAβm is not a pathogenic species responsible for AD (Giuffrida et al., 2009). Recently other small Aβ oligomers, specifically the dimer and the trimer, have been proposed as the species responsible for AD, and the synaptic deficits associated with the disease (Walsh et al., 2002; Cleary et al., 2004; Shankar et al., 2008; Freir et al., 2010). The dimer is found in AD brain but not in brains of stroke patients or patients diagnosed with diseases unrelated to HAβ overproduction (Shankar et al., 2008), and the dimer is correlated with severity of AD dementia (McDonald et al., 2010). Furthermore, synthetic HAβ does not form dimers when the oligomers are prepared under traditional incubations conditions (Dahlgren et al., 2002; Stine et al., 2003) and these oligomers are at least 100-200 fold less potent than naturally secreted HAβ at decreasing long-term potentiation (Wang et al., 2004).

HAβ rapidly inhibits fast axonal transport, however in tau null neurons transport is not inhibited following HAβ treatment (Vossel et al., 2010) suggesting

that HAβ requires tau for its effects on vesicle transport. Between 40 and 70% of the Aβ secreted by neurons is produced following endocytosis of APP (Cirrito et al., 2008). Following endocytosis much of the APP and vesicular Aβ is trafficked to lysosomes and digested after endosome-lysosome fusion (Lorenzen et al., 2010). It has been previously suggested that inhibition of vesicle transport may be one means to generate enhanced Aβ production (Maloney et al., 2005). Thus, we determined if tau-dependent blockage is required to get enhanced RAβ secretion by comparing the levels of secreted RAβ from HAβd/t-treated organotypic hippocampal slices obtained from *TAU*$^{-/-}$ mice and *TAU*$^{-/-}$ mice expressing a human tau transgene. We found no significant differences in RAβ secreted in response to HAβd/t from organotypic slices from either mouse, suggesting that tau-dependent transport inhibition *per se* plays no significant role in HAβd/t-induced RAβ secretion.

Reference List

Alzheimer's Association (2010) Alzheimer's Disease Facts and Figures, *Alzhemiers Dement* 6:158-94

Atwood CS, Perry G, Zeng H, Kato Y, Jones WD, Ling K-Q, Huang X, Moir RD, Wang D, Sayre LM, Smith M, Chen SG, Bush AI (2004) Copper mediates dityrosine cross-linking of Alzheimer's amyloid-beta. *Biochemistry* 43:560-8.

Ausubel FM, Brent R, Kingston RE, Moore DD, Seidman JG, Smith JA, Struhl K (1994) *Current Protocols in Molecular Biology,* Vol 3, Appendix A.1- B.1, John Wiley & Sons, New York.

Bamburg JR, Bloom GS (2009) Cytoskeletal pathologies of Alzheimer disease. *Cell Motil Cytoskeleton* 66:635-49.

Busciglio J, Gabuzda DH, Matsudaira P, Yankner BA (1993) Generation of beta-amyloid in the secretory pathway in neuronal and nonneuronal cells. *Proc Natl Acad Sci USA* 90:2092-6.

Carrodeguas JA, Rodolosse A, Garza MV, Sanz-Clemente A, Pérez-Pé R, Lacosta AM, Domínguez L, Monleón I, Sánchez-Díaz R, Sorribas V, Sarasa M (2005) The chick embryo appears as a natural model for research in beta-amyloid precursor protein processing. *Neuroscience* 134:1285-300.

Castrop H (2010) Genetically modified mice-successes and failures of a widely used technology. *Pflugers Arch* 459:557-67

Cirrito JR, Kang J-E, Lee J, Stewart FR, Verges DK, Silverio LM, Bu G, Mennerick S, Holtzman DM (2008) Endocytosis is required for synaptic activity-dependent release of amyloid-beta in vivo. *Neuron* 58:42-51.

Cleary JP, Walsh DM, Hofmeister JJ, Shankar GM, Kuskowski MA, Selkoe DJ, Ashe KH (2004) Natural oligomers of the amyloid-beta protein specifically disrupt cognitive function. *Nat Neurosci* 8:79-84.

Dahlgren KN, Manelli AM, Stine WB, Baker LK, Krafft G, LaDu MJ (2002) Oligomeric and fibrillar species of amyloid-beta peptides differentially affect neuronal viability. *J Biol Chem* 277:32046-53.

Ehehalt R, Keller P, Haass C, Thiele C, Simons K (2003) Amyloidogenic processing of the Alzheimer beta-amyloid precursor protein depends on lipid rafts. *J Cell Bio* 160:113-23.

Esselmann H, Maler JM, Kunz N, Otto M, Paul S, Lewczuk P, Rüther E, Kornhuber J, Wiltfang J (2004) Lithium decreases secretion of Aβ1-42 and C-truncated species Aβ1-37/38/39/40 in chicken telencephalic cultures but specifically increases intracellular Aβ1-38. *Neurodegener Dis* 1:236-41.

Finder VH, Glockshuber R (2007) Amyloid-beta aggregation. *Neurodegener Dis* 4:13-27.

Freir DB, Fedriani R, Scully D, Smith IM, Selkoe DJ, Walsh DM, Regan CM (2010) Aβ oligomers inhibit synapse remodelling necessary for memory consolidation. *Neurobiol Aging*.

Fukumoto H, Tomita T, Matsunaga H, Ishibashi Y, Saido TC, Iwatsubo T (1999) Primary cultures of neuronal and non-neuronal rat brain cells secrete similar proportions of amyloid beta peptides ending at Aβ40 and Aβ42. *Neuroreport* 10:2965-9.

Fung J, Frost D, Chakrabartty A, McLaurin J (2004) Interaction of human and mouse Aβ peptides. *J Neurochem* 91:1398-403.

Gasparini L, Rusconi L, Xu H, Soldato P del, Ongini E (2004) Modulation of beta-amyloid metabolism by non-steroidal anti-inflammatory drugs in neuronal cell cultures. *J Neurochem* 88:337-48.

Giuffrida ML, Caraci F, Pignataro B, Cataldo S, De Bona P, Bruno V, Molinaro G, Pappalardo G, Messina A, Palmigiano A, Garozzo D, Nicoletti F, Rizzarelli E, Copani A (2009) Beta-amyloid monomers are neuroprotective. *J Neurosci* 29:10582-7.

Glenner GG, Wong CW (1984) Alzheimer's disease: initial report of the purification and characterization of a novel cerebrovascular amyloid protein. *Biochem Biophys Res Commun* 120:885-90.

Goldsbury C, Whiteman IT, Jeong EV, Lim YA (2008) Oxidative stress increases levels of endogenous amyloid-beta peptides secreted from primary chick brain neurons. *Aging Cell* 7:771-5.

Hardy J, Selkoe DJ (2002) The amyloid hypothesis of Alzheimer's disease: progress and problems on the road to therapeutics. *Science* 297:353-6.

Hasegawa T, Ukai W, Jo D, Xu X, Mattson M, Nakagawa M, Araki W, Saito T, Yamada T (2005) Homocysteic acid induces intraneuronal accumulation of neurotoxic Aβ42: Implications for the pathogenesis of Alzheimer's disease. *J Neurosci Res* 80:869–76.

Jankowsky JL, Younkin LH, Gonzales V, Fadale DJ, Slunt HH, Lester HA, Younkin SG, Borchelt DR (2007) Rodent Aβ modulates the solubility and distribution of amyloid deposits in transgenic mice. *J Biol Chem* 282:22707-20.

Johnstone E, Chaney M, Norris F, Pascual R, Little S (1991) Conservation of the sequence of the Alzheimer's disease amyloid peptide in dog, polar bear and five other mammals by cross-species polymerase chain reaction analysis. *Brain Res Mol Brain Res* 10:299-305.

Koo EH, Squazzo SL (1994) Evidence that production and release of amyloid beta-protein involves the endocytic pathway. *J Biol Chem* 269:17386-9.

Krafft G, Klein WL (2010) ADDLs and the signaling web that leads to Alzheimer's disease. *Neuropharmacology* 59:230-42.

Kricka LJ (2002) Stains, labels and detection strategies for nucleic acids assays. *Ann Clin Biochem* 39:114-129.

Lorenzen A, Samosh J, Vandewark K, Anborgh PH, Seah C, Magalhaes AC, Cregan SP, Ferguson SSG, Pasternak SH (2010) Rapid and direct transport of cell surface APP to the lysosome defines a novel selective pathway. *Mol Brain* 3:11.

Marksteiner J, Humpel C (2008) Beta-amyloid expression, release and extracellular deposition in aged rat brain slices. *Mol Psychiatry* 13:939-52.

Mattson MP (2004) Pathways towards and away from Alzheimer's disease. *Nature* 430:631-9.

McDonald JM, Savva GM, Brayne C, Welzel AT, Forster G, Shankar GM, Selkoe DJ, Ince PG, Walsh DM (2010) The presence of sodium dodecyl sulphate-stable Aβ dimers is strongly associated with Alzheimer-type dementia. *Brain* 133:1328-41.

Minamide LS, Striegl AM, Boyle JA, Meberg PJ, Bamburg JR (2000) Neurodegenerative stimuli induce persistent ADF/cofilin-actin rods that disrupt distal neurite function. *Nat Cell Biol* 2:628-36.

Portelius E, Bogdanovic N, Gustavsson MK, Volkmann I, Brinkmalm G, Zetterberg H, Winblad B, Blennow K (2010) Mass spectrometric

characterization of brain amyloid beta isoform signatures in familial and sporadic Alzheimer's disease. *Acta Neuropathol* 120:185-93.

Price DL, Sisodia SS, Gandy SE (1995) Amyloid beta amyloidosis in Alzheimer's disease. *Curr Opin Neurol* 8:268-74.

Shankar GM, Bloodgood BL, Townsend M, Walsh DM, Selkoe DJ, Sabatini BL (2007) Natural oligomers of the Alzheimer amyloid-beta protein induce reversible synapse loss by modulating an NMDA-type glutamate receptor-dependent signaling pathway. *J Neurosci* 27:2866-75.

Shankar GM, Li S, Mehta TH, Garcia-Munoz A, Shepardson NE, Smith I, Brett FM, Farrell MA, Rowan MJ, Lemere CA, Regan CM, Walsh DM, Sabatini BL, Selkoe DJ (2008) Amyloid-beta protein dimers isolated directly from Alzheimer's brains impair synaptic plasticity and memory. *Nat Med* 14:837-42.

Shen C, Chen Y, Liu H, Zhang K, Zhang T, Lin A, Jing N (2008) Hydrogen peroxide promotes Abeta production through JNK-dependent activation of gamma-secretase. *J Biol Chem* 283:17721-30.

Stenh C, Englund H, Lord A, Johansson A-S, Almeida CG, Gellerfors P, Greengard P, Gouras GK, Lannfelt L, Nilsson LNG (2005) Amyloid-beta oligomers are inefficiently measured by enzyme-linked immunosorbent assay. *Ann Neurol* 58:147-50.

Stine WB, Dahlgren KN, Krafft GA, LaDu MJ (2003) In vitro characterization of conditions for amyloid-beta peptide oligomerization and fibrillogenesis. *J Biol Chem* 278:11612-22.

Stoppini L, Buchs PA, Muller D (1991) A simple method for organotypic cultures of nervous tissue. *J Neurosci Methods* 37:173-82.

Suzuki N, Cheung T, Cai X, Odaka A, Otvos L, Eckman C, Golde T, Younkin S (1994) An increased percentage of long amyloid beta protein secreted by familial amyloid beta protein precursor (beta APP717) mutants. *Science* 264:1336-1340.

Tanzi RE, Bertram L (2005) Twenty years of the Alzheimer's disease amyloid hypothesis: a genetic perspective. *Cell* 120:545-55.

Thomas RS, Liddell JE, Murphy LS, Pache DM, Kidd EJ (2006) An antibody to the beta-secretase cleavage site on amyloid-beta-protein precursor inhibits amyloid-beta production. *J Alzheimers Dis* 10:379-90.

Townsend M, Mehta T, Selkoe DJ (2007) Soluble Aβ inhibits specific signal transduction cascades common to the insulin receptor pathway. *J Biol Chem* 282:33305-12.

Townsend M, Shankar GM, Mehta T, Walsh DM, Selkoe DJ (2006) Effects of secreted oligomers of amyloid beta-protein on hippocampal synaptic plasticity: a potent role for trimers. *J Physiol* 572:477-92.

Vossel KA, Zhang K, Brodbeck J, Daub AC, Sharma P, Finkbeiner S, Cui B, Mucke L (2010) Tau reduction prevents Aβ-induced defects in axonal transport. *Science* 330:98.

Walsh DM, Klyubin I, Fadeeva JV, Cullen WK, Anwyl R, Wolfe MS, Rowan MJ, Selkoe DJ (2002) Naturally secreted oligomers of amyloid beta protein potently inhibit hippocampal long-term potentiation in vivo. *Nature* 416:535-9.

Walsh DM, Tseng BP, Rydel RE, Podlisny MB, Selkoe DJ (2000) The oligomerization of Aβ-protein begins intracellularly in cells derived from human brain. *Biochemistry* 39:10831-10839.

Wang Q, Walsh DM, Rowan MJ, Selkoe DJ, Anwyl R (2004) Block of long-term potentiation by naturally secreted and synthetic amyloid β-peptide in hippocampal slices is mediated via activation of the kinases c-Jun N-terminal activated protein kinase as well as metabotropic glutamate receptor type 5. *J Neurosci* 24:3370 -3378.

Xia W, Yang T, Shankar G, Smith IM, Shen Y, Walsh DM, Selkoe DJ (2009) A specific enzyme-linked immunosorbent assay for measuring beta-amyloid protein oligomers in human plasma and brain tissue of patients with Alzheimer disease. *Arch Neurol* 66:190-9.

CHAPTER TWO

AMYLOID BETA DIMERS/TRIMERS POTENTLY INDUCE COFILIN-ACTIN RODS THAT ARE INHIBITED BY MAINTAINING COFILIN PHOSPHORYLATION

Preface and Acknowledgement

The work presented in this chapter was submitted to Molecular Neurodegeneration. The order and list of authors is as follows: Richard C. Davis, Ian T. Marsden, Michael T. Maloney, Laurie S. Minamide, Marcia Podlisny, Dennis J. Selkoe, and J.R. Bamburg. My contributions to the work include: (1) the purification of the Aβ monomer and dimer/trimer from 7PA2 conditioned medium; (2) the quantification of the Aβ secreted by these cells using a dot-blot assay; (3) purification and testing of the dityrosine cross-linked synthetic human $A\beta_{1\text{-}42}$ dimer.

The authors gratefully acknowledge funding from the NIH National Institute of Neurological Disorders and Stroke (NS40371 to J.R.B., NS43115 to RCD, MTM, and JRB) and a Core Infrastructure Grant for Microscope Imaging from Colorado State University. We are grateful for technical assistance of Chi Pak and Alisa Shaw and valuable discussions from these same individuals and from Barbara Bernstein, Kevin Flynn, and O'Neil Wiggan.

Abstract

Previously we showed oligomers of synthetic amyloid beta ($A\beta_{1-42}$) induced cofilin activation and formation of cofilin-actin rods in a neuronal subpopulation of rat hippocampus primarily localized within the dentate gyrus. Here we demonstrate that CHO cell (7PA2) secreted Aβ dimer/trimer (Aβd/t) at ~250 pM is more potent in rod induction in both dissociated hippocampal neuronal cultures and organotypic slices than 1 μM synthetic Aβ as typically prepared oligomers, about a 4000 fold difference. Treatment of the Aβd/t fraction with an Aβ-neutralizing antibody eliminates its rod inducing activity. Traditionally prepared synthetic Aβ oligomers contain SDS-stable trimers and tetramers, but are devoid of dimers. When synthetic human Aβ was incubated under conditions that generate a tyrosine oxidized dimer, the concentration that was required to induce rods decreased dramatically. The oxidized dimer had a maximum rod-inducing activity at ~2 nM (10 ng/mL), suggesting it is the presence of the SDS-stable tyrosine oxidized Aβ dimer in a low-n state that is largely responsible for the potency of the secreted Aβd/t. Aβd/t-induced rods are highly localized to the dentate gyrus and mossy fiber pathway and form more rapidly (significant over controls by 2 h compared to 8 h for those induced by synthetic Aβ-oligomers). Aβd/t-induced rods are reversible, disappearing by 24 h after washout. Cofilin dephosphorylation in response to Aβd/t is greatest within the hippocampal regions of rod formation. Overexpression of cofilin phosphatases slingshot and chronophin increase rod formation when expressed alone and exacerbate rod formation when coupled with Aβd/t treatment both in dissociated neurons and

organotypic slice cultures. Overexpression of the cofilin kinase, LIM kinase 1, inhibits Aβd/t-induced rod formation. Together these data support a mechanism through which Aβd/t produces selective synaptic dysfunction affecting learning and memory at least in part via primary effects on cofilin regulation and rod formation in sensitive hippocampal regions.

Introduction

Proteolytic cleavage of amyloid precursor protein (APP) by β- and γ-secretases gives rise to Aβ peptides ranging in length from 39-43 amino acids (Glenner & Wong, 1984; Hardy, & Selkoe, 2002; Mattson, 2004; Price, et al., 1995; Sisodia & Price, 1995; Tanzi, & Bertram, 2005). Early onset familial AD is linked with high penetrance to mutations that lead to increased production of the most amyloidogenic species, $A\beta_{1-42}$ (Chartier-Harlin et al., 1991; Goate et al., 1991; Murrell et al., 1991; Price et al., 1995). The "amyloid hypothesis" proposes that increasing cerebral accumulation of Aβ over years to decades exacerbates cognitive decline, neurodegeneration, and senile plaque deposition associated with AD. Elevated Aβ can result from mutations or allele expression patterns (or both) that enhance its production/aggregation or decrease its clearance/ degradation (Hardy & Selkoe, 2002).

The concept that different isoforms and/or conformations of Aβ deliver independent signals to neurons is widely supported. Although the term Aβ is used to describe a spectrum of peptide species, the effects of different Aβ peptide species on neuronal function or morphology are not the same (Maloney

& Bamburg, 2007; Heredia et al., 2006). Emphasis has been placed recently on the characterization of small soluble oligomeric forms of Aβ, sometimes referred to as Aβ-derived diffusible ligands (ADDLs) (Kraaft and Klein, 2010). ADDLs are toxic to cultured neurons at nanomolar concentrations (Lambert et al., 1998) and at 500 nM they prevent high frequency stimulation-induced long-term potentiation (LTP) measured from the dentate gyrus in acute hippocampal slices (Wang et al., 2002). Furthermore, ADDLs have been linked to hippocampus-dependent temporal memory deficits in mice. Deletion of the BACE1 gene in Tg6799 mice, expressing mutant forms of human APP and presenilin-1, lowered the concentration of ADDLs to wild type levels and rescued temporal memory deficits, implying a direct role of Aβ formation in memory loss (Ohno et al., 2006; Kimura et al., 2010). ADDLs bind to synaptic sites on cultured hippocampal neurons (Gong et al., 2003; Lacor et al., 2004) where they impair insulin receptor signaling (Zhao et al., 2008) and where stimulation by insulin prevents the pathogenic binding of ADDLs (De Felice et al., 2009).

An even more potent synaptic-inhibitory preparation of Aβ containing SDS-stable dimers and trimers (Aβd/t) has been obtained from culture medium of a CHO cell line (7PA2) expressing a mutant human APP (Walsh et al., 2002). When used at their physiologically relevant (subnanomolar) concentrations to treat hippocampal slices, the Aβd/t fraction and a fraction of Aβ dimer obtained from postmortem human AD brain markedly inhibited the development of long-term potentiation and enhanced long-term depression (LTD), electrophysiological correlates of learning and memory defects in intact animals (Cleary et al., 2005;

Shankar et al., 2008). Single intracerebral ventricular (i.c.v.) infusions into adult rat brain of either gel filtered Aβd/t from 7PA2 cells or Aβ dimer from human AD brain caused transient memory and learning deficits (Walsh et al., 2002; Cleary et al., 2005; Townsend et al., 2006; Shankar et al., 2008; Freir et al., 2010). Infusion (i.c.v.) of Aβd/t into adult rat brain several hours after training inhibits synaptic remodeling that accompanies learning and memory consolidation by preventing a transient increase in the number of synapses in the dentate gyrus (Freir et al., 2010). Although their mechanism is unknown, the SDS-stable Aβd/t or dimer fractions cause synaptic dysfunction at sub-nanomolar concentrations, which are 10^3- 10^4 fold lower than commonly used traditionally prepared oligomeric forms of synthetic Aβ, and 10^2-10^3 fold lower than concentrations of ADDLs. In this regard it is significant that the presence of the SDS-stable Aβ dimer is strongly associated with Alzheimer-type dementia (McDonald et al., 2010).

In addition to the classical hallmarks of AD pathology, amyloid plaques and phospho-tau-containing neuropil threads and neurofibrillary tangles, histopathological structures involving actin and the actin-binding protein, cofilin, have been identified in AD brain (reviewed in Bamburg & Bloom, 2009). Rod-shaped arrays of cofilin-saturated actin bundles (cofilin-actin rods) are induced in cultured hippocampal neurons and organotypic hippocampal slice cultures in response to mitochondrial dysregulation (ATP-depletion) (Minamide et al., 2000; Huang et al., 2008; Davis et al., 2009; Bamburg et al., 2010), oxidative stress (Minamide et al., 2000; Kim et al., 2009), excitotoxic glutamate (Minamide et al.,

2000), extracellular ATP (Homma et al., 2008), overexpression of cofilin (Bernstein et al., 2006), and exposure to Aβ oligomers (Maloney et al., 2005; Davis et al., 2009), each of which is a potential mediator of synaptic loss observed in both familial and sporadic AD (reviewed in Ohm et al., 2007). Rods contain actin and cofilin in a 1:1 complex (Minamide et al., 2010), they form in tandem arrays (striations) within neurites, and they serve as sites for accumulation of phosphorylated tau (Whiteman et al., 2009), suggesting that they may play a role in formation of striated neuropil threads, the major tau pathology in human AD brain (Velasco et al., 1998). Cofilin-actin rods can grow to completely occlude the neurites in which they form (Minamide et al., 2000) and thus inhibit vesicular transport (Maloney et al., 2005; Jang et al., 2005) and cause microtubule loss (Minamide et al., 2000). Because an early indication of AD is blockage in axonal transport that leads to axonal swellings (reviewed in Stokin and Goldstein, 2006; Velasco et al., 1998) and synaptic loss (Davies et al., 1987), we investigated the ability of the physiologically relevant amounts of Aβd/t to induce cofilin activation (dephosphorylation) and rod formation in rat hippocampal neurons and organotypic slices. The Aβd/t dose, time course, reversibility of Aβd/t rod formation, and the location of rods in the hippocampus, all suggest that cofilin-actin rods are likely mediators of Aβd/t in synaptic dysfunction and memory and learning deficits.

Materials and Methods

Reagents

All chemicals are reagent grade and were obtained from Sigma-Aldrich Co. and all tissue culture reagents were from Life Technologies (Invitrogen, Carlsbad, CA). Synthetic Aβ peptide ($A\beta_{1-42}$) and a scrambled peptide with the $A\beta_{1-42}$ amino acid composition were purchased from AnaSpec, Inc. (San Jose, CA). Amyloid beta monomer and dimer/trimer fractions were prepared from the culture medium of CHO 7PA2 cells (Walsh et al., 2002) as previously described (Cleary et al., 2005; Shankar et al., 2007), and unless noted otherwise were used at 1x concentration (equivalent to their secreted concentration in the medium). Similar fractions obtained from culture medium of wild type CHO cells were used as controls.

Culture treatments of dissociated neurons and slices

Synthetic Aβ oligomer was made by solubilizing the peptide in hexafluoroisopropanol and drying in 10 µg aliquots. Each 10 µg of synthetic $A\beta_{1-42}$ was solubilized in 10 µL of DMSO, diluted with 78.6 µL of sterile Ham's F-12 (to yield a 25 µM stock) and incubated 24 h at 4ºC (Dahlgren et al., 2002; Stine et al., 2003; Maloney et al., 2005). Scrambled peptide was prepared identically and both scrambled peptide and synthetic $A\beta_{1-42}$ oligomer were added to a final concentration of 1 µM. The secreted Aβ fractions (monomer or d/t) or the corresponding fractions from control medium, were prepared as described (Cleary et al., 2005), and after gel filtration were freeze-dried to remove the

ammonium acetate buffer. These were reconstituted to 5X or 10X in culture medium and diluted with culture medium to achieve the desired final concentrations. Di-tyrosine oxidized $A\beta_{1-42}$ dimer was prepared from synthetic human $A\beta_{1-42}$ by incubation in the presence of Cu^{2+} and hydrogen peroxide as previously described (Atwood et al., 2004; Barnham et al., 2004; Smith et al., 2007). The oxidized tyrosine dimer Aβ was assayed for rod inducing ability in dissociated neuronal cultures. Treated cultures were placed the incubator for 24-48 h before further treatment or experimentation.

Animals

Timed pregnant Sprague Dawley rats were obtained from Harlan (Indianapolis, IN). E18 fetal rat hippocampal neurons were obtained from timed-pregnant dams and were frozen for future culture work as per published methods (Mattson and Kater, 1988). Pups were sacrificed on postnatal days 6-10 for slice preparation. Animal studies were performed according to the National Research Council's guide for care and use of laboratory animals using protocols approved by the Institutional Animal Care and Use Committee.

Dissociated hippocampal neurons and organotypic slice cultures

Primary hippocampal neurons from E18 rat embryos were prepared and cultured essentially as described (Minamide et al., 2000). Hippocampal slice cultures were prepared from P6-P10 Sprague Dawley rat pups also essentially as described (Stoppini et al., 1991). Briefly, hippocampi were quickly dissected

into filter sterilized ice-cold (4ºC) Gey's Balanced Salt Solution plus 4% glucose, then sliced to a thickness of 400 µm on a McIlwain tissue chopper. Although for some slices we maintained some entorhinal cortex along with the hippocampus to minimize the degeneration of the perforant pathway (Davis et al., 2009), and it made no difference in the results. For most slice treatments, 3-6 slices were arranged onto 0.4 µm Transwell® Polyester membranes inserted into 6 well culture plates (Corning Costar® 3450, Lowell, MA). Beneath the membrane was added 1.7 mL of filter sterilized slice culture medium (50 mL horse serum, 50 mL Hank's Balanced Salt Solution (HBSS), 100 mL Minimal Essential Medium (MEM), 500 µL 1.25 mM L-glutamine, 4 mL 25% glucose, 1 mL 10,000 U/mL Penicillin-Streptomycin). MEM is 4-(2-hydroxyethyl)-1-piperazine ethane sulfonic acid (HEPES) and bicarbonate buffered. Slice culture medium was aspirated and replaced with 1.5 mL of fresh medium on day 3 and every 2-3 days thereafter or with treatment medium as required. For all experiments slices were cultured for about 10 days in a 95% air/5%CO_2 incubator at 35^{o}C.

Hippocampal slices were also cultured on coverslips. Slices (1 or 2) were placed onto 12 x 22 mm coverslips, and embedded in 20 µL of chicken plasma (Cocalico Biologicals, Inc., Reamstown, PA) containing 6 µL of freshly added thrombin (150 NIH units/mL in water; MP Biomedicals, Inc.). Slides were placed hippocampal side up on flat bottom test tubes (Nunclon Delta Tubes, Nalge Nunc, Rochester, NY) and 700 µL slice culture medium was added. Tubes were placed at a 5^{o} angle in a roller incubator (10 revolutions per hour) at 35^{o}C and medium was replaced every 2-3 days.

Immunoblotting

Lyophilized gel filtration fractions of 7PA2 and control culture medium, and synthetic Aβ oligomer preparations were resuspended in 10 µL of 2x sample buffer. For Western blots, samples were electrophoresed on 10–20% acrylamide gradient Tris-Tricine Ready Gels (Bio-Rad, Hercules, CA). Proteins were transferred onto nitrocellulose (0.1 µm; Whatman, Dassel, Germany), the membrane heated to boiling for 10 min in PBS and blocked at room temperature in 1% BSA, 2% goat serum in 20 mM Tris-HCl, pH 7.4, containing 150 mM NaCl (TBS) for 30 min. The primary antibody used was the Aβ monoclonal antibody 6E10 (Covance, Dedham, MA; 1:1000 in TBS plus 0.05% Tween-20 (TBST)), incubated overnight at 4^{o} C.

Approximately 25-33% of a slice containing the dentate gyrus and mossy fiber tract region was microdissected and prepared separately from the remainder of the slice from untreated, Aβd/t-treated or synthetic Aβ-treated cultured hippocampal slices. These were placed in 10 µL of 2X sample preparation buffer (200 mM Tris-HCl pH 6.8, 2% SDS, 40% glycerol, 2% 2-mercaptoethanol, 0.04% Bromophenol Blue), heated to boiling for 3 min, and cooled on ice. Adequate cofilin and phospho-cofilin immunostaining for quantification could be detected on western blots with about 25% of an organotypic slice. Thus, we combined 2-3 dentate gyrus/mossy fiber tract pieces and loaded about 30% of the sample and combined two of the remaining regions and loaded about 20-40% of these samples into wells of a 15% isocratic

Tris/Glycine SDS-gel (Laemmli et al., 1970). Proteins were transferred to PVDF membrane, blocked with 5% milk in TBS and cofilin and phospho-ADF/cofilin were detected using a cofilin monoclonal antibody MAb22 (Abe et al., 1989; 1-2 ng/μL in TBST) and affinity purified rabbit antibody 4321 to phospho-ADF/cofilin (Meberg et al., 1998; 0.1 ng/μL). Primary antibodies were incubated overnight at 4^{o} C.

Secondary antibodies (goat anti-mouse or goat anti-rabbit) conjugated to DyLight 680 or DyLight 800 (1:15,000; Thermo Scientific, Rockford, IL) were added and incubated for 45 min at room temperature. Blots were washed with TBST and bound antibody was visualized with a LI-COR Odyssey Infrared Imaging System. Band intensities were quantified using TotalLab software (Nonlinear Dynamics, Newcastle upon Tyne, UK). For quantitative ratio imaging of total cofilin/ phospho-cofilin, readings were obtained from the same sample on the same blot at the two wavelengths for detection and thus did not require normalization for gel loading. For several samples we also loaded half the amount used for quantification to determine that we were within the linear range of detection (signal intensity decreased by 50% when identical imaging parameters were used).

Aβ was quantified in 7PA2 cell culture medium, combined gel filtration fractions of the 7PA2 medium, synthetic Aβ oligomer preparations, and tyrosine dimers using a dot blot assay with synthetic human β-amyloid peptide ($A\beta_{1-42}$) as a standard. Blots were on nitrocellulose (0.1 μm). Once samples were applied, the membrane was boiled 10 min in PBS to expose epitopes in oligomers and

then Aβ was detected with 6E10 antibody and spots quantified as described above for Western blots.

Adenoviral-mediated gene expression

Adenoviruses for expressing slingshot phosphatase 1L (SSH1L), constitutively active LIM kinase (LIMKT508EE), a dominant negative LIM kinase (D470A) and human cofilin-EGFP have all been described previously (Dawe et al., 2003; Soosairajah et al., 2005; Garvalov et al., 2007). These were used at a multiplicity of infection (m.o.i.) of 100-300 for infecting dissociated neurons. For infection of organotypic slices, about 10^7 adenoviral particles were added directly to the slice culture medium on day 7 and the cultures were returned to the incubator until treated with Aβd/t or control material on day 8 and fixed for analysis on day 10. Slices cultured on membranes were infected with adenovirus by placing a drop of the adenovirus directly on the slice and adding any excess virus to the culture medium below the slice. One to two hours later the liquid on top of the slice was removed and mixed with the culture medium below the slice. This method gave a higher efficiency of infection than if the virus was only added to the medium below the slice

Fixation and immunostaining

Dissociated neurons and slices were fixed for 4 h at room temperature in 4% paraformaldehyde in either cytoskeletal buffer (CBS; 10 mM MES pH 6.1, 138 mM KCl, 3 mM $MgCl_2$, 2 mM EGTA pH 7.0, 4% PEG, 0.32 M sucrose) or

PBS adjusted to pH 7.0, with no apparent differences between buffers. Slices were methanol (-20^{o}C) permeabilized for 10 min and blocked in 2% goat serum/1% bovine serum albumin in Tris-buffered saline before immunostaining. Primary antibodies include: affinity purified rabbit 1439 IgG to chick ADF (2 ng/μL), which cross-reacts with mammalian ADF and cofilin (Shaw et al., 2004), protein A purified monoclonal mouse anti-cofilin (MAb22; 10 ng/μL IgG) (Abe et al., 1989), affinity purified rabbit IgG to the phosphorylated peptide of chick ADF (rabbit 4321; 1 ng/μL) (Meberg et al., 1998), and mouse monoclonal antibody to actin (clone C4; ICN Biomedicals, Inc., Costa Mesa, CA). Secondary antibodies, all used at 1:450, include fluorescein goat anti-rabbit and goat anti-mouse and Texas-Red goat anti-rabbit and goat anti-mouse (Molecular Probes, Eugene, OR). DAPI (4'-6-Diamidino-2-phenylindole) or Hoechst 33342 were used to stain DNA. After blocking and staining, slices on membrane were cut out and mounted on 22 x 22 mm cover glasses with ProLong Gold Antifade (Molecular Probes).

Microscopy and Image analysis

An Olympus IX81 microscope equipped with an ASI piezo stage (Applied Scientific Instrumentation, Eugene, OR), CSU22 spinning disk confocal head (Yokogawa Instruments, Japan), 440 nm, 473 nm and 561 nm diode lasers, and a 1Kx1K Cascade II EMCCD Camera (Roper Scientific, Tucson, AZ), all integrated and operated by SlideBook software (Intelligent Imaging Innovations, Denver, CO), was used to obtain confocal sections through organotypic slices.

The objectives used include 4x Fluorite (0.13 NA), UAPO40X/340W-DIC (1.35 NA), or PlanAPO 60x (1.42 NA).

Phase-contrast and non-confocal fluorescence micrographs were obtained on a Nikon Diaphot using 4x (0.13 NA), 10x (0.25 NA), 20x (0.75 NA) air objectives or 40x (1.3 NA), 60x (1.4 NA), 100x (1.4 NA) oil. For experiments in which we localized active cofilin across an entire slice, fixed slices were immunostained for phospho-ADF/cofilin (rabbit antibody 4321) and total cofilin (mouse MAb22), stained with different fluorescently tagged secondary antibodies, and imaged using the 4x objective, which allowed capture of most of the hippocampal area in one field. The two images were overlaid (total cofilin/phospho-cofilin) and a hot scale applied to the ratio image such that the hottest colors correspond to the regions of most active (dephosphorylated) cofilin.

MetaMorph v7.03 software (MDS Analytical Technologies, Toronto, Canada) was used for all digital processing. Following time-lapse imaging the slice was scanned for rod formation. All experiments were repeated a minimum of three times. To ascertain the regional distribution of rods, the total number of rods per field was counted using a 60x oil objective and data from multiple slices were combined onto a schematic of the hippocampus as described previously (Davis et al., 2009).

Statistics

Statistical analyses were done with either MATLAB or SPSS v13. All significance values are at $p<0.05$ and all error bars are standard deviations unless otherwise stated. Any post hoc tests are reported.

Results

Amyloid beta dimer/trimer is a potent inducer of cofilin-actin rods

SDS-PAGE and Western blot analysis of the amyloid beta (Aβ) immunoreactive components in fractions of 7PA2 culture medium demonstrated separation of monomer from a fraction enriched in dimer/trimer (Aβd/t) (fraction 12-13, Figure 2.1A). Treatment of cultured dissociated hippocampal neurons with the Aβd/t fraction at 1X concentration (1X = the equivalent concentration produced in the CHO 7PA2 cell culture medium) induced cofilin-actin rods in many neurons, similar to treatment with 1μM of synthetic Aβ oligomers (Figure 2.2). Significant rod induction did not occur in neurons treated with either the Aβ monomer fraction (e.g. fraction 15, Figure 2.1A) or fraction 12-13 prepared from medium of wild type CHO cells (non-conditioned (NC) medium). Incubation of Aβd/t or synthetic Aβ oligomer with an anti-Aβ monoclonal antibody (6E10) for 15 min prior to neuronal treatment reduced rod formation to control levels, strongly suggesting it is Aβ and not some other component of the 7PA2 culture medium

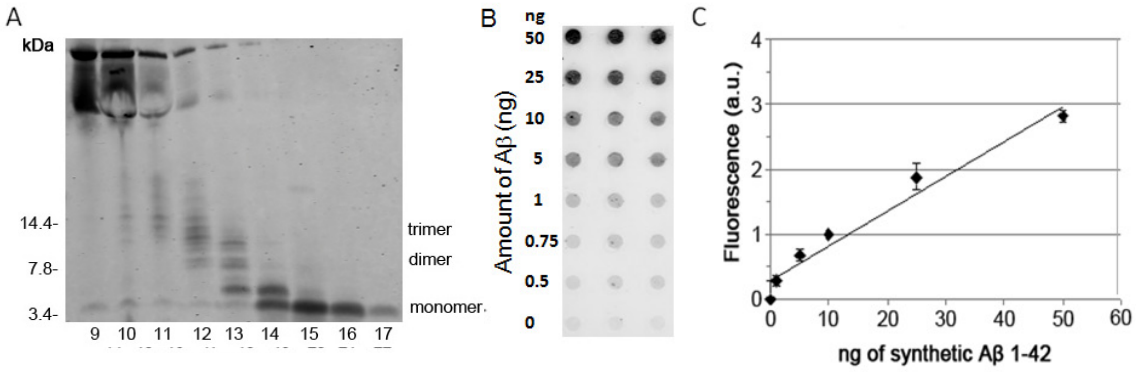

Figure 2.1: Preparation and quantification of Aβd/t. (A) Aβ Western blot (6E10 antibody) of gel filtration fractions from a single Superdex75 (10/30 HR) column run at a flow rate of 0.5 mL/min and loaded with 1 mL of a 10X concentrate of 7PA2 cell conditioned (16 h) DMEM medium (Cleary et al., 2005; Shankar et al., 2007). (B, C) Dot blot standard curve for quantification of Aβ monomer equivalents in the 7PA2 culture medium and final Aβd/t fraction.

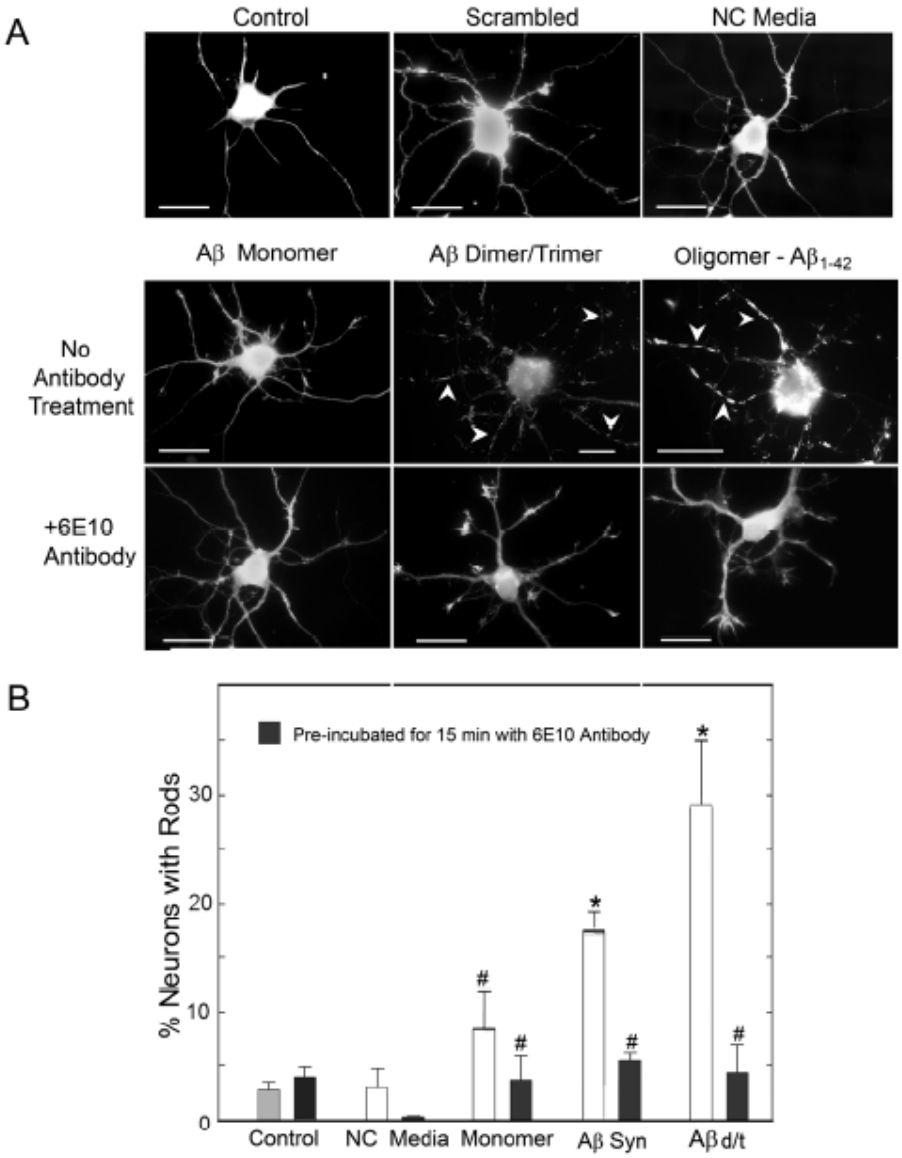

Figure 2.2: Aβd/t fraction from 7PA2 cells, but not monomer, induces rods in dissociated hippocampal neurons. Analysis by fluorescence microscopy of dissociated neurons treated with vehicle (control), scrambled Aβ peptide (1 μM), or nonconditioned (NC media, d/t equivalent fraction), as well as with the monomer and d/t fractions from 7PA2 cell culture medium and synthetic Aβ oligomers (Aβsyn). (A) Cofilin immunostained fluorescence images of hippocampal neurons showing representative responses with cofilin-actin rods formed 24 h after treatment with Aβd/t- and Aβsyn treated neurons. Pretreatment of the Aβ-fractions with an antibody (6E10) to Aβ eliminates their rod-inducing effects. Bars = 10 μm. (B) Quantification of the rod forming response showing the neutralizing effects of the 6E10 antibody and the non-significant changes in rod formation by Aβ monomer. (* = $p < 0.05$ compared to control; # not significantly different from control).

that is responsible for inducing rods. The percentage of neurons with rods was quantified from each of the cultures treated with fractionated NC medium, monomeric Aβ, the Aβd/t fraction, and synthetic Aβ oligomer (Figure 2.2B). Only the Aβd/t fraction and synthetic Aβ oligomers induced a significant ($p<0.01$) increase in the percentage of neurons with rods above untreated (or synthetic scrambled peptide-treated) controls. Pretreatment with 6E10 antibody eliminated this increase. Furthermore, the percentage of Aβd/t-treated neurons forming rods (about 30%) represents a significant ($p<0.05$) increase versus treatment with the 1 μM synthetic Aβ oligomers (18%).

The total concentration of Aβ species in 7PA2 conditioned medium was previously reported to be 6.4 ng/mL (1.4 nM) based on ELISA (Cleary et al., 2005). However, oligomers of human Aβ are inefficiently measured by ELISA (Stenh et al., 2005). Therefore we measured the total Aβ concentration in several batches of 7PA2 medium using a dot blot assay and obtained the value of 8.3 ± 0.8 ng/mL (s.d.) (Figure 2.1). The amount of Aβd/t and Aβm in 1X fractions were also determined directly from dot blot assays to be approximately 1.1 ng/mL and 3.6 ng/mL, respectively, equal to about 250 pM and 800 pM based on monomer content (there was some variability from preparation to preparation depending on the fractions pooled). Our Aβd/t concentration values are very close to those estimated from the Aβd/t immunostaining on Western blots after epitope exposure by boiling the membrane (Cleary et al., 2005), and are also quite similar to the amounts of Aβd/t estimated by Freir et al. (2010).

We next compared the Aβd/t fraction to the synthetic Aβ oligomer for their dose-response in rod-induction. The gel filtration fractions elute in 50 mM ammonium acetate, pH 8.5 and are freeze dried to remove most of the volatile buffer. However, when reconstituted they cannot be used above a 2.5X concentration because of increased cell death (release of LDH, data not shown). However, neurons could be treated with these fractions from 0.1X to 2X without any significant cell loss over 48 h. One control for Aβd/t is an identically treated volume of culture medium from wild type CHO cells. As shown in Fig. 2.3A, the half maximal response in terms of numbers of neurons forming rods is achieved with about 0.4X Aβd/t (~100 pM) and ~0.7 μM synthetic Aβ oligomers, about a 7000 fold difference between the half-maximal responses. This value compares favorably with a more conservative 4000 fold difference obtained with the single point comparison at 1X concentration (250 pM Aβd/t versus 1 μM synthetic oligomer), which gives near maximal rod response for each preparation. Furthermore, the maximum percentage of cells with rods is about 10% greater with the Aβd/t than with the synthetic Aβ oligomers at all but the lowest concentrations used.

When synthetic human Aβ was incubated under conditions that generate a tyrosine oxidized dimer, the concentration that was required to induce rods decreased dramatically. The oxidized dimer had a maximum rod-inducing activity at ~2 nM (10 ng/mL), suggesting it is the presence of the SDS-stable tyrosine oxidized Aβ dimer in a low-n state that is largely responsible for the potency of the secreted Aβd/t.

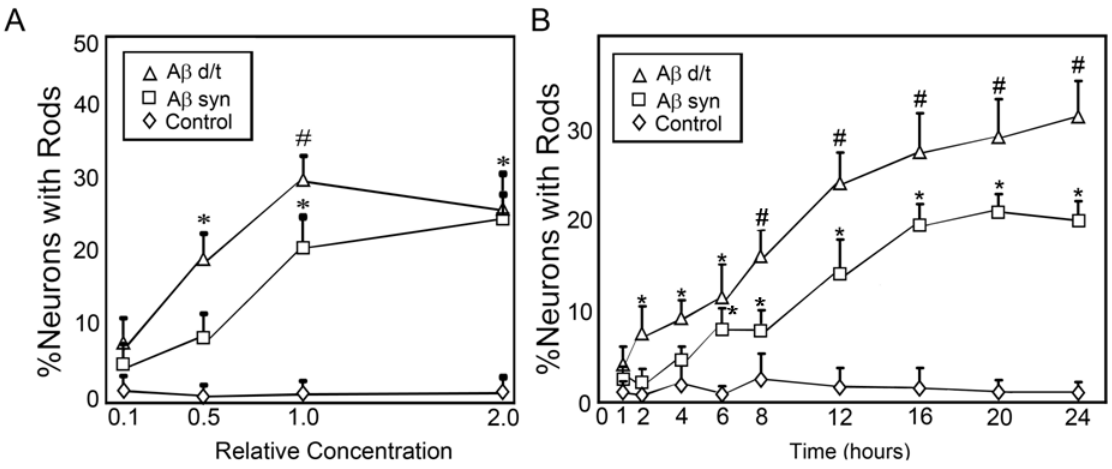

Figure 2.3: Percent of neurons in dissociated hippocampal cultures containing rods as a function of Aβ form, concentration and time of treatment. (A) Dose-response curves for Aβsyn and Aβd/t versus control. The concentrations are expressed in terms of the 7PA2 CHO cell secreted concentration of Aβd/t (1X), which was used at 0.1, 0.5 and 2X this value. For the synthetic Aβ oligomers, the 1X value equals 1.0 μM. (B) Following treatment with 1X amounts of Aβd/t or Aβ synthetic oligomer, neurons were fixed at the times shown and the percent of neurons with rods was quantified. By 2 h the percent of neurons forming rods in response to Aβd/t was significant (*) over controls ($p<0.05$). The Aβsyn-treated neurons required 6 h to reach significance over controls. Significance (# = $p<0.05$) in the differences between the two Aβ species occurred at 8 h.

Time course of rod formation

We previously observed that the percentage of neurons forming rods in response to 1 μM synthetic Aβ oligomers did not increase significantly over untreated samples until 6 h after addition (Maloney et al., 2005). Because the Aβd/t fraction is more active in rod induction than synthetic Aβ, we directly compared the time course between these two treatments. The 1X Aβd/t fraction induces a measurable but not significant increase in rods over untreated controls by 1 h becoming significant ($p<0.05$) by 2 h, at which time about 25% of the maximum response is obtained (Figure 2.3B). Although 1 μM synthetic Aβ oligomer increased rod induction over the untreated controls by 4 h, the increase did not become significant until 6 h as previously observed (Maloney et al., 2005). By 8 h significantly ($p<0.05$) more Aβd/t-treated neurons have rods than neurons treated with synthetic Aβ oligomer and this difference is maintained through 24 h.

Stability of the added Aβd/t fraction

To determine if the Aβd/t fraction added to the cultured organotypic slices underwent a change in concentration or altered its SDS-stable dimer/trimer form during the incubation, we removed culture medium at the end of experiments (48 h) and human Aβ was immunoprecipitated and reanalyzed by SDS-PAGE (Figure 2.4).

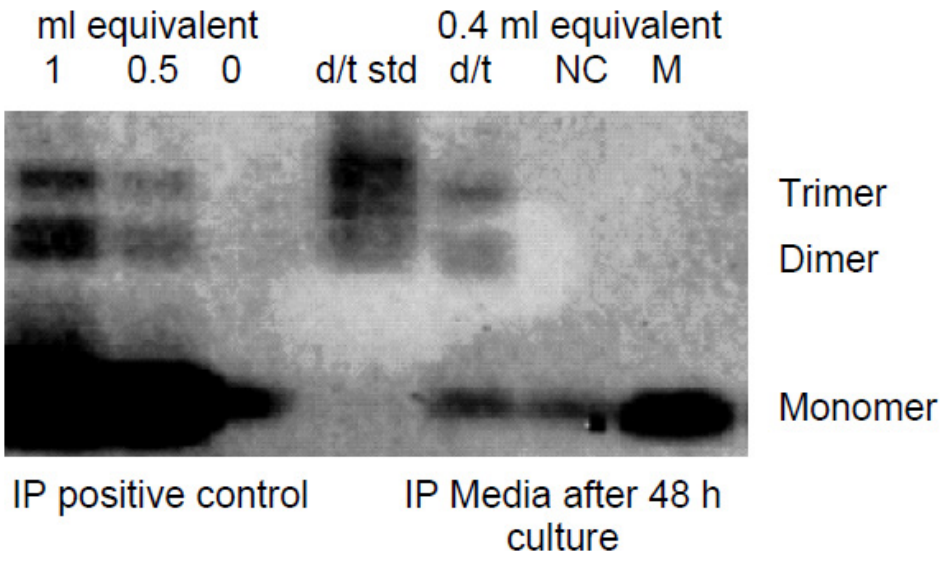

Figure 2.4: The Aβd/t fraction remains stable for 48 h when incubated with neurons. Immunoprecipitates from 7PA2 medium (IP positive controls on left) and from neuronal culture medium 48 h after treatment with Aβd/t, the equivalent fraction from NC medium, or the monomer fraction. The load volume on the right is equivalent to 0.4 mL of starting 7PA2 medium and the dimer/trimer bands are slightly less than what is contained in the 0.5 mL of starting medium showing that the d/t fraction is stable over the 48 h of culture.

Regional analysis of rod formation in slices

The numbers of rods in fields taken from multiple organotypic hippocampal slices treated 48 h with 1X Aβd/t fraction or with control treatments used above were mapped onto a matrix grid of the hippocampus using fiduciary points to stretch and fit multiple slice data onto a single summary map as previous described (Davis et al., 2009). Similar to the localization of rods in response to synthetic Aβ (Davis et al., 2009), a treatment also repeated here (data not shown), the Aβd/t-induced rods were mainly localized to the polymorphic hilar region of the dentate gyrus and along the mossy fiber tract into the CA3 region (Figure 2.5). Furthermore, the numbers of rods per grid square is on average 2-3 fold higher than for the comparable region of the slices treated with synthetic Aβ oligomer (not shown, but compare numbers on hot scale in Figure 2.5A with the top scale of 15 rods per square previously published for synthetic Aβ-treated slices (Davis et al., 2009)). Rod numbers in slices treated with the gel filtration fraction of NC CHO cell medium were not significantly different from untreated controls and thus data from these slices were combined to make the control panel (Figure 2.5A). Similar to what was observed in dissociated neurons (Figure 2.2B), pretreatment of Aβd/t with 6E10 antibody reduced the rod numbers in slices to control levels (data not shown).

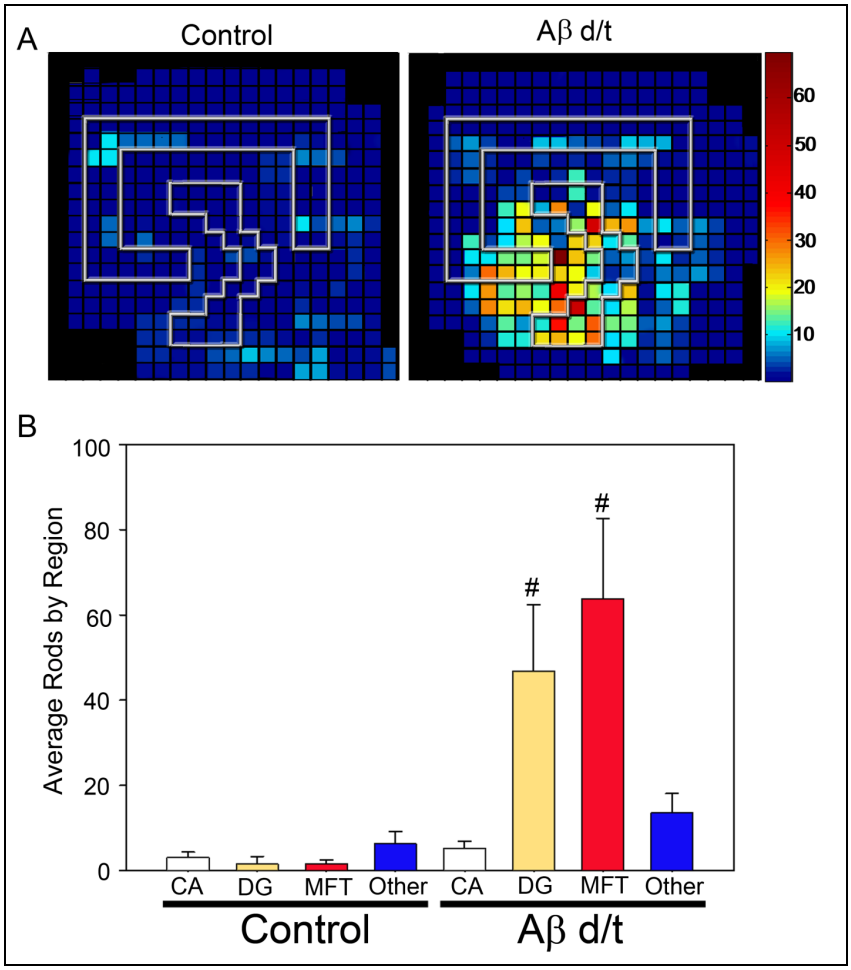

Figure 2.5. Numbers of rods induced by Aβd/t are highest in neurons within the dentate gyrus and mossy fiber tract in organotypic hippocampal slices. (A) Organotypic hippocampal slices were cultured for at least 8-10 days and were left untreated or treated with 1X Aβd/t, the same amount of the equivalent NC medium fraction, or scrambled Aβ peptide. After 48 h, slices were fixed and immunostained for cofilin and DNA (DAPI), and rods were quantified by counting with a 60x objective. Rod mapping from multiple slices onto a matrix grid of the hippocampus was performed as previously described using fiduciary markers from the stained nuclei layers to align hippocampal regions (Davis et al., 2009). There were no differences detected in rod numbers or distribution between the untreated slices and those treated with NC medium or scrambled peptide and these were all combined to give the control panel. Rods induced by the Aβd/t were heavily concentrated over the dentate gyrus and mossy fiber tract. (n = 18 for control slices and n = 12 for Aβd/t treated). (B) Rod quantification averaged per field over different regions of the slices. Each field acquired with the 60x objective has about 6-7 matrix grid squares. The only regions of significance (# = $p<0.05$) for the rod numbers are in the dentate gyrus and mossy fiber tract.

Dose response curves for rod induction in organotypic slices

We compared the dose-response curves for rod formation in response to Aβd/t and synthetic Aβ oligomers in organotypic slice cultures by quantifying rods per field (Figure 2.6A). It should be noted that one field encompasses the equivalent of about 6-7 matrix grid squares and that rod counts were averaged over the entire slice. Surprisingly, slices treated with the Aβd/t fraction at 0.1X (estimated to be 25 pM) have a significant ($p<0.05$) increase in rods per field over controls, equivalent to the numbers of rods per field induced by 500 nM synthetic Aβ oligomer. The curves are very similar to the dose-response measured in dissociated neuronal cultures and quantified as percent of neurons with rods (Figure 2.3).

Rods induced by Aβd/t are reversible

To test if rods induced in organotypic slices by Aβd/t are reversible, the Aβd/t was washed out 24 h after treatment and slices were allowed to recover for 24 h in control medium. As previously demonstrated for rods induced by synthetic Aβ (Davis et al., 2009), the majority of rods induced by 1X Aβd/t disappear 24 h after washout (Figure 2.6B).

Cofilin dephosphorylation is induced by Aβd/t

We evaluated the changes in cofilin phosphorylation levels in response to Aβd/t-treatment of organotypic slices using both Western blotting and fluorescence ratio imaging for total cofilin/phospho-cofilin in slices (Figure 2.7).

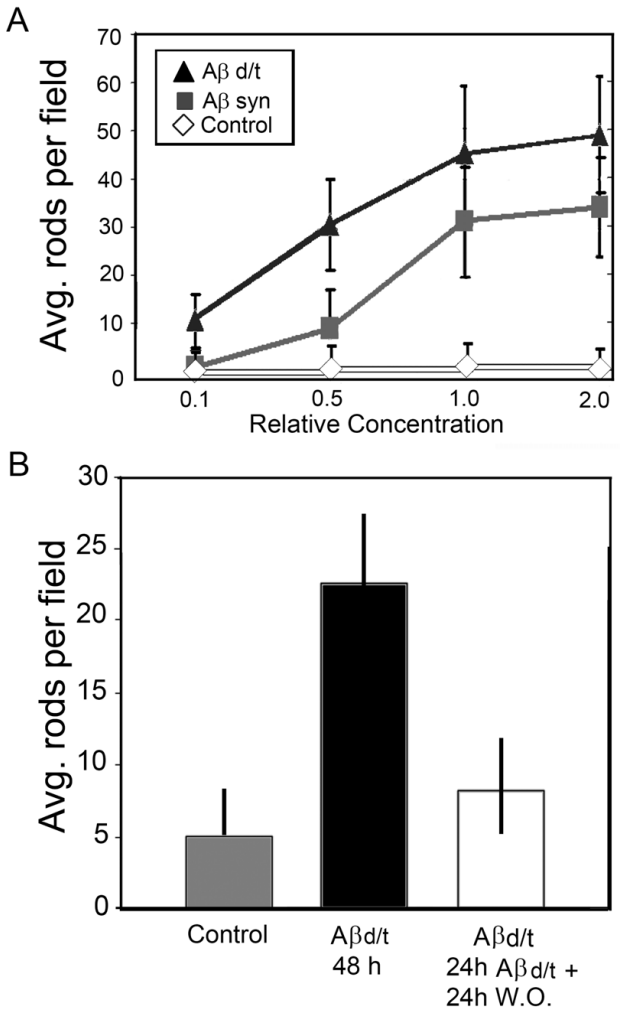

Figure 2.6. Dose-response curve for rod formation in organotypic hippocampal slices and reversibility of Aβd/t-induced rods. (A) The same concentrations of Aβd/t and synthetic oligomer used in Figure 2.3A were applied to organotypic hippocampal slices. After 48 h, slices were fixed and rods immunostained and quantified per field averaged across the entire slice. The curves obtained are very similar to those in dissociated neurons but the measured parameters are different (average rods per field measured here vs. percent neurons with rods in Figure 2.3A). (B) Rods formed in response to Aβd/t in hippocampal slices reached their maximum value by 24 h (see Figure 2.3B). To determine rod reversibility, some of the slices were washed free of the Aβd/t and allowed to incubate another 24 h, whereas others had the Aβd/t present continuously. Controls were treated with the NC medium for 48 h or were left untreated (no difference). As previously shown for the rods induced by synthetic Aβ oligomers (Davis et al., 2009), the Aβd/t-induced rods are also reversible.

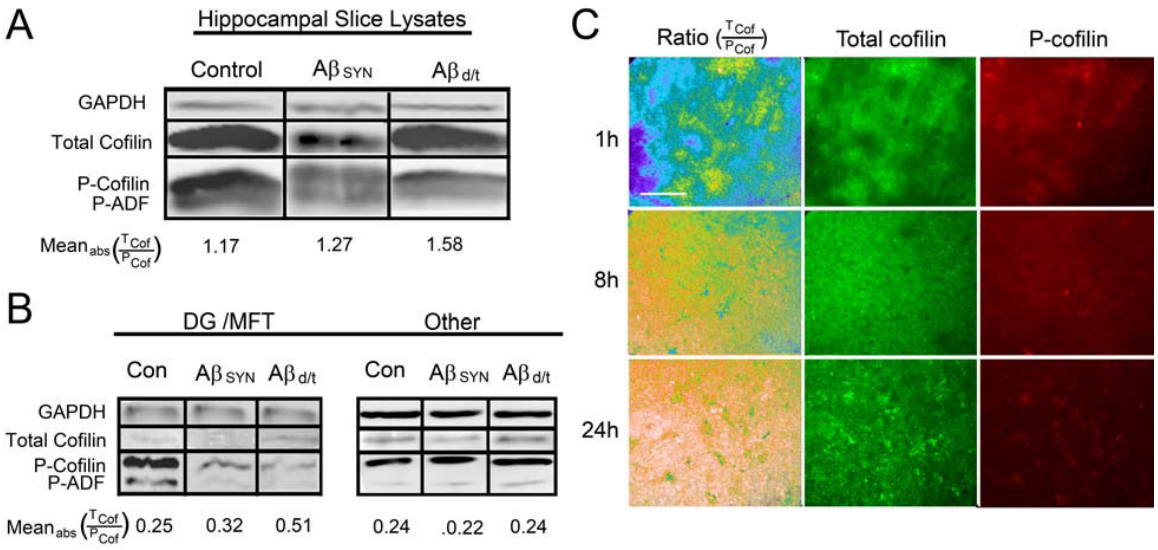

Figure 2.7. Aβd/t induces cofilin dephosphorylation (activation) within the hippocampal region where rods are most abundant. (A, B) Western blots of extracts from whole slices (A) and microdissected slice regions (B) from either untreated (controls) or slices treated with Aβsyn or Aβd/t. Blots were stained for GAPDH (loading control), total cofilin (MAb22 antibody) and phospho-ADF/cofilin (rabbit antibody). The ratio of the immunostaining for total cofilin/phospho-cofilin showed that in whole slices (A) there was a slight (1.08 fold) increase in cofilin dephosphorylation following Aβsyn treatment and a larger (1.35 fold) increase in slices treated with the Aβd/t (n = 3 slices). (B) In the microdissected regions containing the dentate gyrus and mossy fiber tract the Aβsyn treatment increased cofilin dephosphorylation by 1.28 fold and the Aβd/t increased it by 2.04 fold. The remainder of the slice regions (other) showed no significant change in phospho-cofilin levels. (C) Ratio imaging of the total cofilin/phospho-ADF/cofilin immunostained slices also show a time dependent enhanced cofilin dephosphorylation that is localized over the dentate gyrus and mossy fiber tract (shown in the images here) but not elsewhere in the slices. Maximum ratio (white in hot scale) is set at 2. At this low magnification, only the largest of the rods are visible. Phospho-cofilin is excluded from rods. Bar = 50 μm.

The phospho-cofilin antibody also detects phospho-ADF equally well but ADF is expressed at only about 20% of the level of cofilin in the rat brain and phospho-ADF declines similarly to phospho-cofilin (Figure 2.7B). Immunoblots of whole slices show a slight decline in phospho-ADF/cofilin when treated with 1 μM synthetic Aβ oligomer and a greater decline when treated with 1X Aβd/t (Figure 2.7A) as indicated by the increased total cofilin/phospho-cofilin ratio. However, when regions of the hippocampus were micro-dissected for immunoblotting, larger changes in the ratio are observed in extracts from the dentate gyrus than from the remainder of slice (Figure 2.7B) and Aβd/t-treatment gave the greater rod-inducing response in this region. Similar conclusions are reached by observing the fluorescence ratio images of total cofilin/phospho-ADF/cofilin staining of slices at 1, 8 and 24 h after treatment (Figure 2.7C). The greatest changes were observed in the dentate gyrus shown in Figure 2.5C, where there was no quantifiable difference between the 0 (not shown) and 1 h time point, but a significant increase in the ratio (about 50% of maximum change) was observed by 8 h, similar to the time course for rod formation observed in Figure 2.3B.

Rods are not very apparent in the low magnification images used for slice ratio imaging (Figure 5C), but become apparent when viewed with a 60x objective, even in single confocal sections (Figure 2.8A). However, the rod distribution and abundance within the dentate gyrus are more impressive when the confocal image stack is deconvolved and the lowest 20% intensity of immunstaining is removed by resetting the low threshold on an image histogram (Figure 2.8B). Only a few densely stained cofilin aggregates are observed in

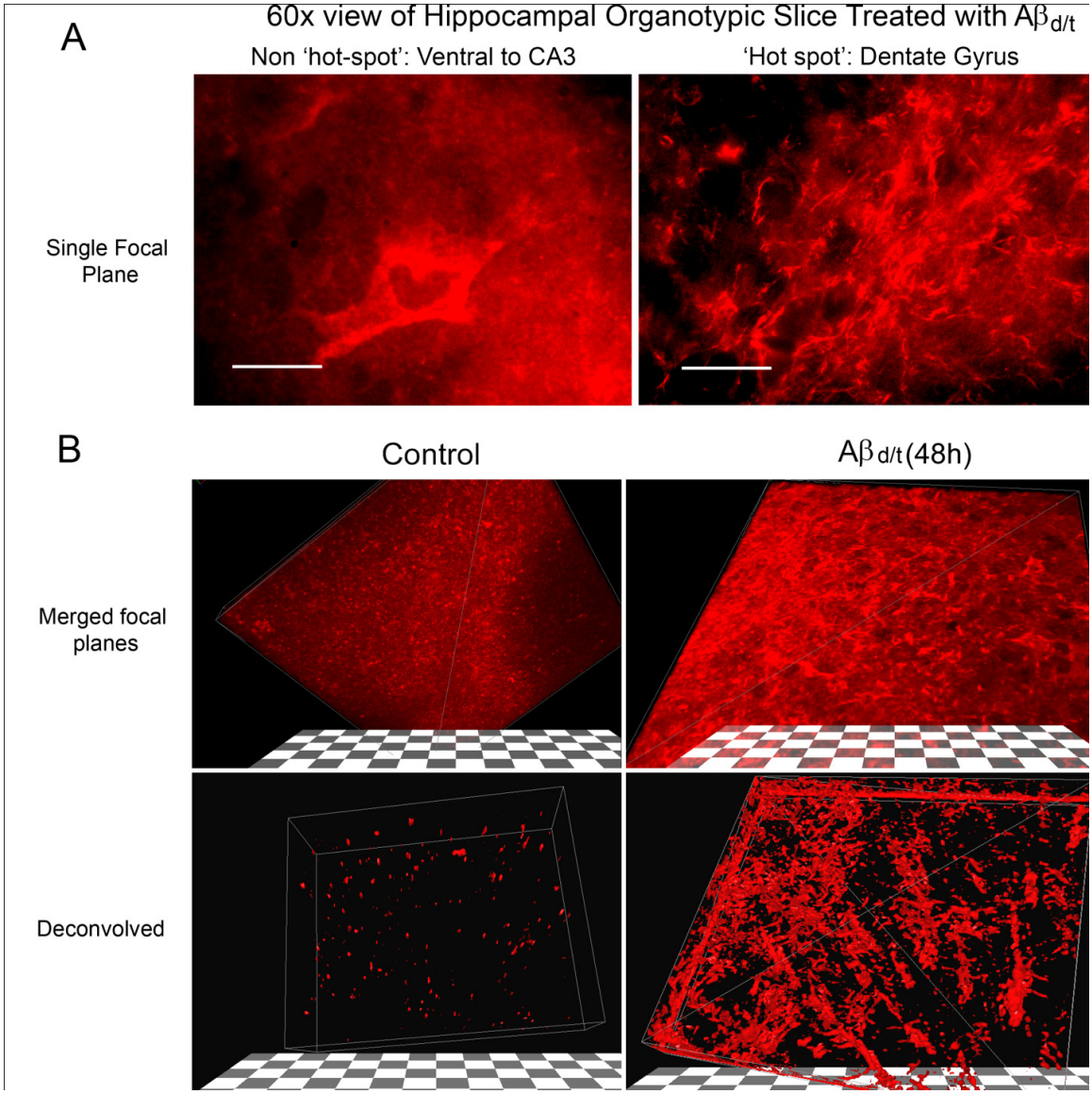

Figure 2.8. Three-dimensional reconstruction of cofilin-stained rods in deconvolved confocal image stacks from organotypic slices. Treatment of organotypic slices with Aβd/t results in a profound increase in cofilin immunostained rods in the dentate gyrus/mossy fiber tract (DG/MFT) and a global change in cofilin distribution in cells in this region. (A) Single focal plane of non-rod-forming region near the CA3 compared to a rod hot spot in the dentate gyrus. Rods are evident in this single plane. (B) Three dimensional stack of planes from a cofilin stained control and Aβd/t-treated slice. Deconvolution of the confocal image stacks and thresholding the image by removing the lowest 20% of signal (lower panels) provides striking evidence of rod formation in this region. Hundreds of rods can be observed, which contain virtually all of the remaining immunostained cofilin.

the 3D reconstruction of the image stack from control slices whereas rods are abundant throughout the Aβd/t-treated slice.

Modulating cofilin phosphorylation alters rod formation and response to Aβ oligomers

Since rod formation correlates well with cofilin dephosphorylation, we examined the effects of enhancing or inhibiting cofilin dephosphorylation on rod formation in untreated dissociated neuronal cultures or those treated with synthetic Aβ oligomer. Adenoviral-mediated expression of the cofilin phosphatases, either slingshot (SSH1L) or chronophin (CIN), but not their inactive forms, increases rod formation in the absence of any other rod-inducing treatment whereas the inactive form of slingshot (C393S) appears to act in a dominant negative manner by reducing rod formation in Aβd/t-treated cells (Figure 2.9A). Fluorescent protein co-expression allowed us to identify the infected cells and score these independently from the uninfected cells in the same culture. Greater than 15% of neurons overexpressing SSH1L formed rods, the most dramatic effect observed, whereas about 8% of neurons expressing CIN formed rods. Treating neurons expressing these cofilin phosphatases with Aβ significantly ($p<0.05$) enhanced rod formation above the levels induced by the Aβ-treatment alone to a maximum of 38% for the SSH-1L expressing neurons; expressing the dominant negative form of SSH1L kept the number of neurons forming rods in response to Aβd/t to less than 10%.

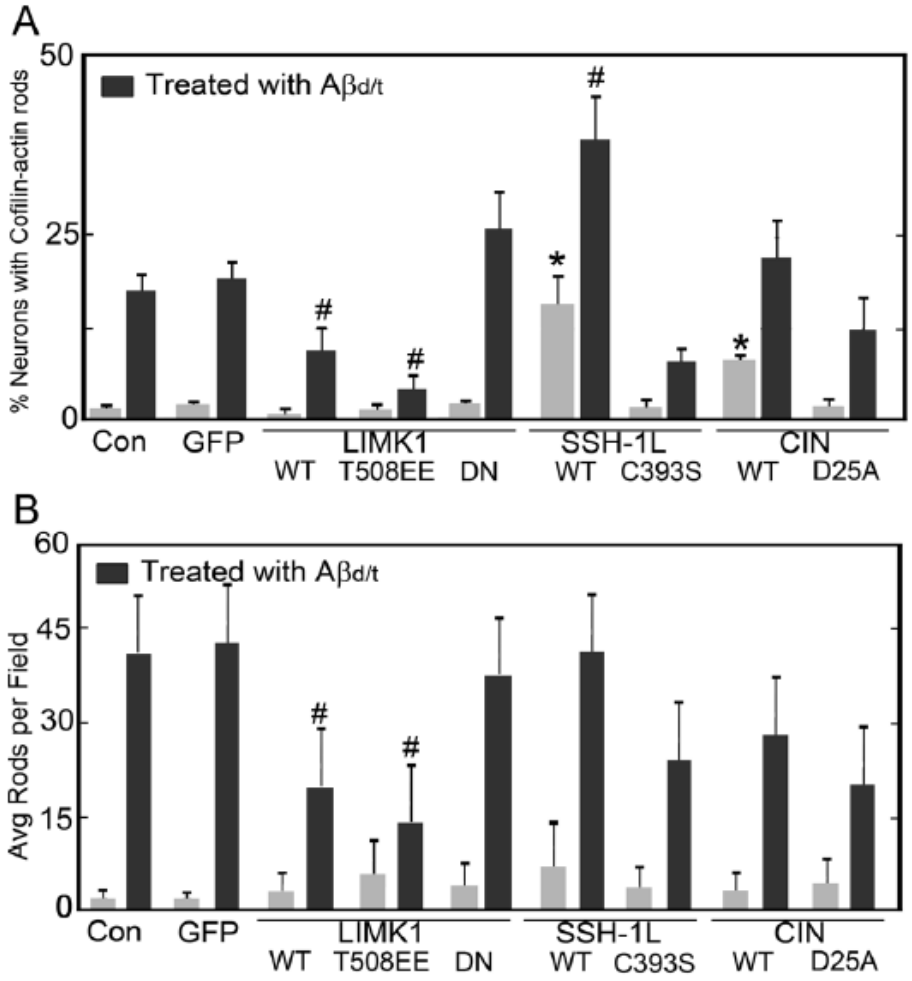

Figure 2.9. Upstream regulators of cofilin phosphorylation impact the ability of Aβd/t to induce rods. Rod formation was quantified in (A) dissociated hippocampal neuronal cultures or (B) organotypic hippocampal slices that were uninfected (Con), infected with control adenovirus expressing GFP (GFP) or with adenoviruses expressing various upstream regulators of cofilin phosphorylation. All viruses coexpressed a fluorescent protein marker and only neurons expressing the marker were scored in the dissociated cultures. In slices, infection rates were approximately 70% (see Figure 2.10) and rods per field were quantified (it was not possible in slices to count rods only within infected neurons). Neurons or slices were infected 24 h prior to treatment with Aβd/t and were fixed and analyzed for rod formation 48 h after Aβd/t addition. Treatments that enhanced cofilin dephosphorylation (the active phosphatases SSH-1L WT and CIN WT) in the dissociated cultures enhanced rod formation with or without Aβd/t treatment (* = significant difference from untreated or GFP controls at $p<0.05$; # significantly different from Aβd/t treated controls, $p<0.05$). Treatments that inhibited cofilin dephosphorylation (LIMK1 WT and the active LIMK1T508EE), inhibited rod formation in response to Aβd/t in both dissociated neuronal cultures and in slices (n = 3 to 9).

Expression of a dominant negative LIM kinase, the major cofilin kinase, did not alter rod formation when expressed on its own, however its presence enhanced the percent of neurons forming rods in response to Aβd/t, although the difference (from 19-20% to 26%) is not significant at $p<0.05$. The opposite effect was observed upon expression of the wild type or constitutively active form of LIMK1 (LIMKEE508). LIMK1 expression reduced the percent of neurons forming Aβ-induced rods by about 50% for wild type and over 75% for the constitutively active LIMKEE508 and these values are significant at $p<0.05$ (Figure 2.9A).

A similar series of experiments were done using organotypic slices (Figure 2.9B). To first estimate the efficiency of transgene expression in the cells of organotypic slices by adenoviral infection, we examined slices at high magnification after adenoviral-mediated expression of a fluorescent protein and staining of nuclei with DAPI. We quantified the number of nuclei with surrounding fluorescent protein expression (Figure 2.10) and determined a >70% infection efficiency when we used 10^7 infectious particles/slice (based upon a titer of infectious particles per mL obtained by expression of the viral E2b gene in infected cells; Minamide et al., 2003). In organotypic slices, expression of SSH1L or CIN alone did not significantly increase rod formation (quantified as rods per field using the 60x objective) over controls. In addition, we did not observe a rod response to Aβd/t in infected slices that was greater than for Aβd/t-treated controls with any viral-mediated protein expression. However, in slices infected with virus for expressing LIMK wt and LIMK508EE, the average rod number per field in response to Aβd/t was reduced (Figure 2.9B), similar to what

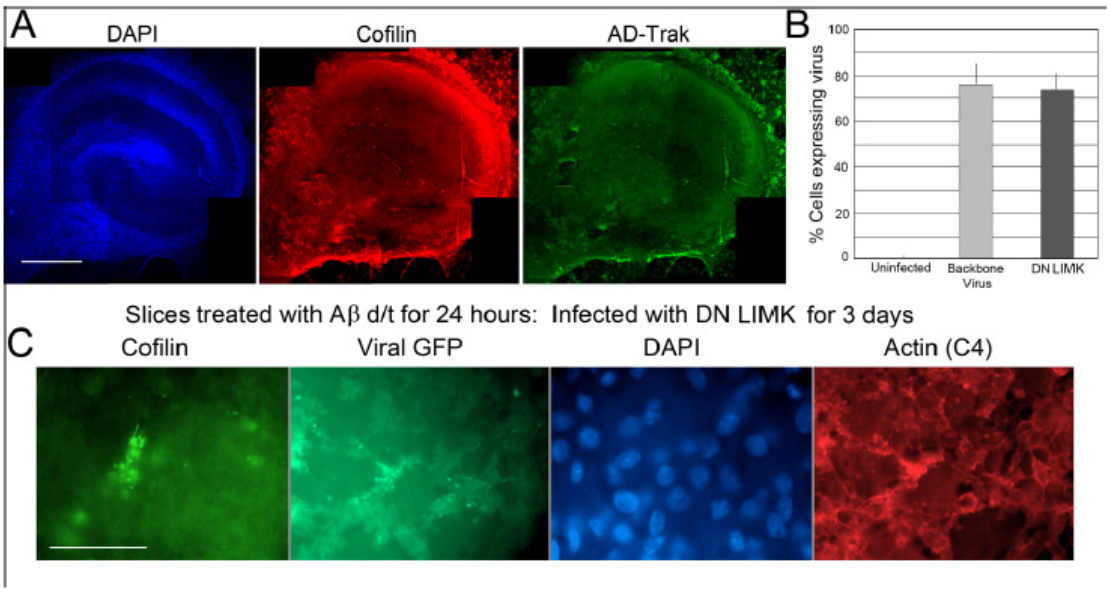

Figure 2.10. (A) Low power images of a hippocampal organotypic slice stained with DAPI, immunostained for cofilin, and imaged for GFP-expression after infection with adenovirus expressing GFP behind a CMV promoter. (B) Comparison of infected cells in organotypic slices, measured by the numbers of cells showing GFP fluorescence around a DAPI stained nucleus (from either GFP control virus or DNLIMK1 AdTrack virus). Between 70-75% of the cells so examined were positive for GFP. (C) This panel was assembled to illustrate how we determined the percentage of infected cells. One region from a confocal plane of an image stack is shown. Staining for cofilin and actin are not important to the quantification of infectivity. The areas surrounding nuclei within this plane were examined for expression of GFP, which had to be above a threshold level for counting as positive. The nuclei were often above or below the optical section of the cell that contained the GFP and we had to move up and down single planes in Z series to obtain the most accurate counts. Many hundreds of nuclei across different areas of the slice were examined to obtain the infection efficiency.

we observed in dissociated cells (Figure 2.9A). Taken together, these results suggest that cofilin dephosphorylation is both necessary and sufficient to induce rod formation in many neurons but that the total rod response is enhanced by Aβd/t-induced stress.

Discussion

Here we demonstrate that the dimer/trimer fraction of a naturally secreted form of Aβ is several thousand fold more active at inducing cofilin-actin rods than traditionally oligomerized samples of synthetic Aβ. This level of activity for Aβd/t (250 pM) is within its estimated physiological concentrations based upon the amounts extracted from human AD brain (Shankar et al., 2008). Because the rod-inducing activity of the Aβd/t fraction is neutralized with an Aβ antibody, it is clearly Aβ that is the active rod-inducing component. Furthermore, the Aβ monomer fraction does not induce rods (not significant above control), suggesting the dimer is the minimal active unit in promoting cofilin-actin rod formation. At optimal concentrations of each, Aβd/t induces formation of rods in more hippocampal neurons than synthetic Aβ oligomers. The Aβd/t also induces more rods per neuron based upon the rod counts per field taken across organotypic slices and mapped from multiple slices onto a hippocampal matrix using the methods we previously described (Davis et al., 2009). Because naturally secreted Aβ is cut from the APP by γ-secretase and has more variability in the peptide lengths that will comprise its mixture, it is certainly possible that there are some specific mixtures of peptide lengths that generate different rod-

inducing ability. However, the fact that the monomer fraction from secreted Aβ is not rod inducing, suggests that it is the process of oligomerization per se that differs for naturally produced and synthetic Aβ.

At the μM concentrations typically used to make oligomers, synthetic Aβ assembles rapidly (Hung et al., 2008) and virtually no SDS-stable dimer remains, although SDS-stable trimers and tetramers are present (e.g. Puzzo et al., 2008), suggesting that the dimer may be the major rod-inducing form. . Picomolar levels of the dimer-deficient synthetic Aβ oligomers enhance LTP, opposite to the effects of the dimer enriched fractions, but a finding that perhaps helps explain the normal physiological function of Aβ. It is not known what specific types of SDS-stable cross-linking occurs in the naturally secreted Aβ dimer, but it has been previously shown that tyrosine10 in the human Aβ sequence can undergo oxidation to form a di-tyrosine cross-link. Because this tyrosine residue is missing in rodent Aβ (phe in place of tyr), and rodent Aβ is deficient in oligomerization (Atwood et al., 2004; Marksteiner and Humpel, 2008), we investigated the biological activity of copper-peroxide oxidized Aβ that is di-tyrosine cross linked (Atwood et al., 2004; Barnham et al., 2004). When synthetic human Aβ was incubated under conditions that generate a tyrosine oxidized dimer, the concentration that was required to induce rods decreased dramatically. The oxidized dimer had a maximum rod-inducing activity at ~2 nM (10 ng/mL), suggesting it is the presence of the SDS-stable tyrosine oxidized Aβ dimer in a low-n state that is largely responsible for the rod-inducing potency of the secreted Aβd/t.

We found that the amount of the Aβd/t remained fairly constant in the medium over 3 d. This is due in part to the fact that rodent Aβ does not oligomerize and hence the continued secretion of Aβ by the cultured neurons, which is even stimulated by the presence of the human Aβd/t (Chapter 1), does not contribute to the Aβd/t pool. It also suggests that uptake of the Aβd/t either does not occur, or if it does occur it must be released again into the medium and not degraded by the cell.

Enhancing cofilin activity by overexpressing either of the cofilin phosphatases slingshot or chronophin, enhanced rod formation in dissociated neurons in the absence of Aβ-treatment and expression of LIMK1 inhibited formation of rods even after Aβ-treatment. This result was not unexpected since simple overexpression of cofilin, especially the non-phosphorylatable cofilin S3A mutant, enhances rod formation (Bernstein et al., 2006). Expression of LIMK1 in organotypic slices reduced rod formation similar to its effect in dissociated neurons, but we did not see a significant increase in rods due to expression of either cofilin phosphatase. Although we find about a 70% adenoviral infectivity rate of cells in the slices, it is quite likely that the non-neuronal cells infect better than the neurons and thus for some viruses the neuronal infectivity may be low enough that we would have difficulty in obtaining enough infected neurons to observe significant changes in rod formation.

Single infusions into the adult rat brain of either Aβ dimer extracted from human AD brain or Aβd/t at the identical concentration used in our studies caused transient memory and learning deficits when measured starting 2 h after

infusion, and completed within a 2 h maximum time frame (Cleary et al., 2005; Shankar et al., 2008). Memory and learning deficits disappeared 24 h after the single infusions. It is worthy to note in this regard that the Aβd/t fraction induces rods in a statistically significant number of neurons by 2 h after treatment (about 25% of the maximal response) and that the Aβd/t rods are reversible, disappearing by 24 h after washout. Thus, formation and disappearance of rods in cultured neurons and organotypic slices correlate well with the changes observed in memory and learning in whole animals exposed to a single infusion of Aβd/t.

Nevertheless, there are some discrepancies in time of rod formation in response to Aβd/t treatment that do not correlate well with acute Aβd/t effects on slice electrophysiology. Decreased long-term potentiation (LTP) and enhanced long-term depression (LTD) occur within 20 min of treating hippocampal slices in culture either with fractions containing Aβd/t (Townsend et al., 2006) or with Aβ dimer extracted from human AD brain (Shankar et al., 2008). This response is more rapid than the 2 hours it takes to obtain a significant increase in rods in organotypic slices exposed to the Aβd/t fraction. Rod formation has been observed to occur within 10 min in organotypic slice cultures responding to anoxia or ATP-depletion (Minamide et al., 2000; Davis et al., 2009). However, the rate of Aβd/t induced rod formation in organotypic slices maintained in neurobasal/B27 medium may be significantly slower than in acute slices prepared for electrophysiology and maintained in artificial cerebrospinal fluid (aCSF) owing to 0.6 μM insulin in the neurobasal/B27 medium not present in

aCSF. Insulin helps neurons resist the pathogenic changes in cytoskeletal organization induced by Aβ (De Felice et al., 2009). Alternatively or in addition, we suspect that cofilin dephosphorylation and altered actin dynamics in response to Aβd/t is rapid and precedes rod formation in some compartments, such as dendritic spines. Synaptic activity depends directly on cofilin function in regulating actin dynamics and may reflect early changes in plasticity (Shankar et al., 2007; Carlisle et al., 2008; Yuen & Yan, 2009; Gu et al., 2010). Thus, the LTP/LTD response to Aβd/t could be independent of rod formation yet the result of a localized change in cofilin activity. Significantly, wash out of Aβ after the electrophysiological changes have occurred did not result in any reversal in the altered LTP/LTD over 2 h. This persistent effect could arise within the organotypic slice from relatively tight binding of the Aβd/t to specific sites for which some evidence does exist (Townsend et al., 2006; De Felice et al., 2009). Alternatively, rod formation may have occurred by the time washout was initiated and rods could be responsible for the lack of rapid recovery. Rods sequester most of the cofilin (Minamide et al., 2000; Bernstein et al., 2006) needed to reestablish the balance in spine actin dynamics (Gu et al., 2010) and their formation would resist rapid recoveries of the spine cofilin pool.

The most sensitive pool of neurons forming rods in response to both synthetic Aβ oligomers and Aβd/t are those within the polymorphic/hilar region of the dentate gyrus along the mossy fiber tract into the CA3. The dentate gyrus is considered to play a central role in associative memory (Morris, 2006). Its major input comes via the perforant pathway with axons representing approximately

one million excitatory entorhinal neurons from layer II. These axons end preferentially within the outer two thirds of the superficial molecular layer, mainly on the apical dendrites of the granule cells, but also on dendrites of interneurons (Ohm, 2007). Cholinergic neurons from the basal forebrain provide another important afferent input, and also synapse with neurons of the dentate gyrus inner molecular layer. The CA3 pyramidal cells receive the granule cell output via the mossy fibers (granule cell axons) and aid in pattern completion (Nakazawa et al., 2002). Because of its central role in associative memory, the dentate gyrus has been extensively studied in AD brain (Ohm, 2007). There is an early loss of synapses (48% decrease in synapse to neuron ratio) before significant loss of neurons (Davies et al., 1987; Bertoni-Freddari et al., 1996; Scheff and Price, 2003). Based upon the degree of immunofluorescence labeling for the synaptic marker synaptophysin, there is a direct correlation of synaptic loss during AD progression. Early, mild and severe AD cases are accompanied by a decline in synaptophysin staining of about 25, 45 and 65%, respectively, in the outer and middle third of the molecular layer, with little to no loss in the inner third (Masliah et al., 1994). Injection of single doses of Aβd/t-containing medium into brains of adult rats also leads to defects in associative memory and to memory consolidation with a striking inhibition of the synaptic increases that occur during memory consolidation in the dentate gyrus (Freir et al., 2010). Because cofilin-actin rod formation in response to Aβd/t is so prominent within the DG and mossy fiber tract, and the rods block transport and cause distal atrophy in the neurites in which they form without death of the

neuron (Minamide et al., 2000; Jang et al., 2005), they represent a likely mechanism to explain the synaptic loss associated with early stages of AD and thus represent a novel target for therapeutic intervention.

Reference List

Abe H, Ohshima S, Obinata T (1989) A cofilin-like protein is involved in the regulation of actin assembly in developing skeletal muscle. *J Biochem* 106:696-702.

Atwood CS, Perry G, Zeng H, Kato Y, Jones WD, Ling K-Q, Huang X, Moir RD, Wang D, Sayre LM, Smith M, Chen SG, Bush AI (2004) Copper mediates dityrosine cross-linking of Alzheimer's amyloid-beta. *Biochemistry* 43:560-568.

Bamburg JR, Bloom GS (2009) Cytoskeletal pathologies of Alzheimer disease. *Cell Motil Cytoskel* 66:635-649.

Bamburg JR, Bernstein BW, Davis RC, Flynn KC, Goldsbury C, Jensen JR, Maloney MT, Marsden IT, Minamide LS, Pak CW, Shaw AE, Whiteman IT, Wiggan O (2010) ADF/cofilin-actin rods in neurodegenerative diseases. *Curr Alzheimer Res* 7:241-250.

Barnham KJ, Haeffner F, Ciccotosto GD, Curtain CC, Tew D, Mavros C, Beyreuther K, Carrington D, Masters CL, Cherny RA, Cappai R, Bush AI. (2004) Tyrosine gated electron transfer is key to the toxic mechanism of Alzheimer's disease beta-amyloid, *FASEB J* 18:1427-1429.

Bernstein BW, Chen H, Boyle JA, Bamburg JR (2006) Formation of actin-ADF/cofilin rods transiently retards decline of mitochondrial potential and ATP in stressed neurons. *Am J Physiol Cell Physiol* 291:C828-C839.

Bertoni-Freddari C, Fattoretti P, Casoli T, Caselli U, Meier-Ruge W (1996) Deterioration threshold of synaptic morphology in aging and senile dementia of Alzheimer's type. *Anal Quant Cytol Histol* 18:209-213.

Busciglio J, Lorenzo A, Yankner BA (1992) Methodological variables in the assessment of beta amyloid neurotoxicity. *Neurobiol Aging* 13, 609-612.

Calderwood DA, Shattil SJ, Ginsberg MH (2000) Integrins and actin filaments: reciprocal regulation of cell adhesion and signaling. *J Biol Chem* 275: 22607-22610.

Carlisle HJ, Manzerra P, Marcora E, Kennedy MB(2008) SynGAP regulates steady-state and activity-dependent phosphorylation of cofilin. *J Neurosci* 28:13673-13683.

Cataldo AM, Petanceska S, Peterhoff CM, Terio NB, Epstein CJ, Villar A, Carlson EJ, Staufenbiel M, Nixon RA (2003) APP gene dosage modulates endosomal abnormalities of Alzheimer's disease in a segmental trisomy 16 mouse model of down syndrome. *J Neurosci* 23:6788-6792.

Chartier-HarlinM C, Crawford F, Hamandi K, Mullan M, Goate A, Hardy J, Backhovens H, Martin JJ, Broeckhoven CV (1991a) Screening for the beta-amyloid precursor protein mutation (APP717: Val----Ile) in extended pedigrees with early onset Alzheimer's disease. *Neurosci Lett* 129:134-135.

Chartier-Harlin MC, Crawford F, Houlden H, Warren A, Hughes D, Fidani L, Goate A, Rossor M, Roques P, Hardy J, Mullan M (1991b) Early-onset Alzheimer's disease caused by mutations at codon 717 of the beta-amyloid precursor protein gene. *Nature* 353:844-846.

Cleary JP, Walsh DM, Hofmeister JJ, Shankar GM, Kuskowski MA, Selkoe DJ, Ashe KH (2005) Natural oligomers of the amyloid-beta protein specifically disrupt cognitive function. *Nat Neurosci* 8:79-84.

Dahlgren KN, Manelli AM, Stine WB, Jr., Baker LK, Krafft GA, LaDu MJ (2002) Oligomeric and fibrillar species of amyloid-beta peptides differentially affect neuronal viability. *J Biol Chem* 277:32046-32053.

Davies CA, Mann DMA, Sumpter PQ, Yates PO (1987) A quantitative morphometric analysis of the neuronal and synaptic content of the frontal and temporal cortex in patient with Alzheimer's disease. *J Neurol Sci* 78:151-164.

Davis RC, Maloney MT, Minamide LS, Flynn KC, Stonebraker MA, Bamburg JR. (2009) Mapping cofilin-actin rods in stressed hippocampal slices and the role of cdc42 in amyloid β-induced rods. *J Alzheimers Dis* 18, 35-50

Dawe HR, Minamide LS, Bamburg JR, Cramer LP (2003) ADF/cofilin controls cell polarity during fibroblast migration. *Curr Biol* 13:252-257.

De Felice FG, Vieira MNN, Bomfim TR, Decker H, Velasco PT, Lambert MP, Viola KL, Zhao WQ, Ferreira ST, Klein WL (2009) Protection of synapses against Alzheimer's-linked toxins: Insulin signaling prevents the pathogenic binding of Aβ oligomers. *Proc Nat Acad Sci USA* 106:1971-1976.

Deshpande A, Mina E, Glabe C, Busciglio J (2006) Different conformations of amyloid beta induce neurotoxicity by distinct mechanisms in human cortical neurons. *J. Neurosci* 26:6011-6018.

Freir DB, Fedriani R, Scully D, Smith IM, Selkoe DJ, Walsh DM, Regan CM (2010) Aβ oligomers inhibit synapse remodelling necessary for memory consolidation. *Neurobiol Aging*. 2010 Jan 22 [Epub ahead of print]

Giancotti FG, Ruoslahti E (1999) Integrin signaling. *Science* 285:1028-1032.

Glenner GG, Wong CW (1984) Alzheimer's disease: initial report of the purification and characterization of a novel cerebrovascular amyloid protein. *Biochem Biophys Res Commun* 120: 885-890.

Goate A, Chartier-Harlin MC, Mullan M, Brown J, Crawford F, Fidani L, Giuffra L, Haynes A, Irving N, James L, Mant R, Newton P, Rooke R, Roquis P, Talbot C, Pericak-Vance M, Roses A, Williamson R, Rossor M, Owen M, Owen M, Hardy J (1991) Segregation of a missense mutation in the amyloid precursor protein gene with familial Alzheimer's disease. *Nature* 349:704-706.

Gong Y, Chang L, Viola KL, Lacor PN, Lambert MP, Finch CE, Krafft GA, Klein WL (2003) Alzheimer's disease-affected brain: presence of oligomeric A beta ligands (ADDLs) suggests a molecular basis for reversible memory loss. *Proc Natl Acad Sci USA* 100:10417-10422.

Grace EA, Busciglio J (2003) Aberrant activation of focal adhesion proteins mediates fibrillar amyloid beta-induced neuronal dystrophy. *J Neurosci* 23:493-502.

Grace EA, Rabiner CA, Busciglio J (2002) Characterization of neuronal dystrophy induced by fibrillar amyloid beta: implications for Alzheimer's disease. *Neuroscience* 114:265-273.

Gu J,Lee CW, Fan Y, Komols D, Tang X, Sun C, Chen G, Yu K, Hartzell HC, Bamburg JR, Zheng JQ (2010) ADF/cofilin-mediated actin dynamics regulate AMPA receptor trafficking during synaptic plasticity. *Nat Neurosci* 13:1208-1215

Hardy J, Selkoe DJ (2002) The amyloid hypothesis of Alzheimer's disease: progress and problems on the road to therapeutics. *Science* 297 353-356.

He TC, Zhou S, da Costa LT, Yu J, Kinzler KW, Vogelstein B (1998) A simplified system for generating recombinant adenoviruses. *Proc Natl Acad Sci USA* 95, 2509-2514.

Heredia L, Helguera P, de Olmos S, Kedikian G, Sola VF, LaFerla F, Staufenbiel M, de Olmos J, Busciglio J, Caceres A, Lorenzo A (2006) Phosphorylation of actin-depolymerizing factor/cofilin by LIM-kinase mediates amyloid beta-induced degeneration: a potential mechanism of neuronal dystrophy in Alzheimer's disease. *J Neurosci* 26:6533-6542.

Homma K, Niino Y, Hotta K, Oka K (2008) Ca(2+) influx through P2X receptors induces actin cytoskeleton reorganization by the formation of cofilin rods in neurites. *Mol Cell Neurosci* 37:261-270.

Huang TY, Minamide LS, Bamburg JR, Bokoch GM (2008) Chronophin mediates an ATP-sensing mechanism of cofilin dephosphorylation and neuronal

cofilin-actin rod formation. *Dev Cell* 15:691-703.

Hung LW, Ciccotosto GD, Giannakis E, Tew DJ, Perez K, Masters CL, Cappai R, Wade JD, Barnham KJ (2008) Amyloid-beta peptide (Aβ) neurotoxicity is modulated by the rate of peptide aggregation: Abeta dimers and trimers correlate with neurotoxicity. *J Neurosci* 28:11950-11958.

Jang DH, Han JH, Lee SH, Lee YS, Park H, Lee SH, Kim H, Kaang BK (2005) Cofilin expression induces cofilin-actin rod formation and disrupts synaptic structure and function in Aplysia synapses. *Proc Natl Acad Sci USA* 102:16072-16077.

Kim JS, Huang TY, Bokoch GM (2009) Reactive oxygen species (ROS) regulate a slingshot-cofilin activation pathway. *Mol Biol Cell* 20:2650-2660.

Kimura R, Devi L, Ohno M (2010) Partial reduction of BACE1 improves synaptic plasticity, recent and remote memories in Alzheimer's disease transgenic mice. *J Neurochem* 113:248-261.

Krafft GA, Klein WL (2010) ADDLs and the signaling web that leads to Alzheimer's disease. *Neuropharmacology* 59:230-42.

Lacor PN, Buniel MC, Chang L , Fernandez SJ, Gong Y, Viola KL, Lambert MP, Velasco PT, Bigio EH, Finch CE, Krafft GA, Klein WL (2004) Synaptic targeting by Alzheimer's-related amyloid beta oligomers. *J Neurosci* 24:10191-10200.

Lambert MP, Barlow AK, Chromy BA, Edwards C, Freed R, Liosatos M, Morgan TE, Rozovsky I, Trommer B, Viola K, Zhang C, Finch CE, Krafft GA, Klein WL (1998) Diffusible, nonfibrillar ligands derived from Aβ-42 are potent central nervous system neurotoxins. *Proc Natl Acad Sci USA* 95:6448-6453.

Maloney MT, Minamide LS, Kinley AW, Boyle JA, Bamburg JR (2005) Beta-secretase-cleaved amyloid precursor protein accumulates at actin inclusions induced in neurons by stress or amyloid beta: a feedforward mechanism for Alzheimer's disease. *J Neurosci* 25:11313-11321.

Masliah E, Mallory M, Hansen L, Deteresa R, Alford M, Terry R (1994) Synaptic and neuritic alterations during the progression of Alzheimer's disease. *Neurosci Lett* 174:67-72.

Mattson MP (2004) Pathways towards and away from Alzheimer's disease. *Nature* 430:631-639.

Mattson MP, Kater SB (1988) Isolated hippocampal neurons in cryopreserved long-term cultures: development of neuroarchitecture and sensitivity to NMDA. *Int J Dev Neurosci* 6:439-452.

McDonald JM, Savva GM, Brayne C, Welzel AT, Forster G, Shankar GM, Selkoe DJ, Ince PG, Walsh DM (2010) The presence of sodium dodecyl sulphate-stable Aβ dimers is strongly associated with Alzheimer-type dementia. *Brain* 133:1328-1341.

Meberg PJ, Ono S, Minamide LS, Takahashi M, Bamburg JR (1998) Actin depolymerizing factor and cofilin phosphorylation dynamics: response to signals that regulate neurite extension. *Cell Motil Cytoskeleton* 39:172-190.

Minamide LS, Striegl AM, Boyle JA, Meberg PJ, Bamburg JR (2000) Neurodegenerative stimuli induce persistent ADF/cofilin-actin rods that disrupt distal neurite function. *Nat Cell Biol* 2:628-636.

Minamide LS, Shaw AE, Sarmiere PD, Wiggan O, Maloney MT, Bernstein BW, Sneider JM, Gonzalez JA, Bamburg JR (2003) Production and use of replication-deficient adenovirus for transgene expression in neurons. *Methods Cell Biol* 71:387-416.

Minamide LS, Maiti S, Boyle JA, Davis RC, Coppinger JA, Bao Y, Huang TY, Yates J, Bokoch GM, Bamburg JR (2010) Isolation and characterization of cofilin-actin rods from stressed cells. *J Biol Chem* 285:5450-5460.

Morris RGM (2006) Elements of a neurobiological theory of hippocampal function: the role of synaptic plasticity, synaptic tagging and schemas. *Eur J Neurosci* 23:2829-2846.

Murrell J, Farlow M, Ghetti B, Benson MD (1991) A mutation in the amyloid precursor protein associated with hereditary Alzheimer's disease. *Science* 254:97-99.

Nakazawa K, Quirk MC, Chitwood, RA, Watanabe M, Yeckel MF, Sun LD, Kata A, Carr CA, Johnston D, Wilson MA, Tonegawa S (2002) Requirement for hippocampal CA3 NMDA receptors in associative memory recall. *Science* 297:211-218.

Ohm TG (2007) The dentate gyrus in Alzheimer's disease. *Prog Brain Res* 163:723-740.

Ohno M, Chang L, Tseng W, Oakley H, Citron M, Klein WL, Vassar R, Disterhoft JF (2006) Temporal memory deficits in Alzheimer's mouse models: rescue by genetic deletion of BACE1. *Eur J Neurosci* 23:251-260.

Price DL, Sisodia SS, Gandy SE (1995) Amyloid beta amyloidosis in Alzheimer's disease. *Curr Opin Neurol,* 8:268-274.

Puzzo D, Privitera L, Leznik E, Fa M, Staniszewski A, Palmeri A, Arancio O (2008) Picomolar amyloid-beta positively modulates synaptic plasticity and memory in hippocampus *J Neurosci* 28:14537-45.

Scheff SW, Price DA (2003) Synaptic pathology in Alzheimer's disease: a review of ultrastructural studies. *Neurobiol Aging* 24:1029-1046.

Shankar GM, Bloodgood BL, Townsend M, Walsh DM, Selkoe DJ, Sabatini BL (2007) Natural oligomers of the Alzheimer amyloid-beta protein induce reversible synapse loss by modulating an NMDA-type glutamate receptor-dependent signaling pathway. *J Neurosci* 27:2866-2875.

Shankar GM, Li S, Mehta TH, Garcia-Munoz A, Shepardson NE, Smith I., Brett FM, Farrell MA, Rowan MJ, Lemere CA, Regan CM, Walsh DM, Sabatini BL, Selkoe DJ (2008) Amyloid-beta protein dimers isolated directly from Alzheimer's brains impair synaptic plasticity and memory. *Nat Med* 14:837-842.

Shaw AE, Minamide LS, Bill CL, Funk JD, Maiti S, Bamburg JR (2004) Cross-reactivity of antibodies to actin- depolymerizing factor/cofilin family proteins and identification of the major epitope recognized by a mammalian actin-depolymerizing factor/cofilin antibody. *Electrophoresis* 25:2611-2620.

Sisodia SS, Price DL (1995) Role of the beta-amyloid protein in Alzheimer's disease. *FASEB J* 9:366-370.

Smith DG, Cappai R, Barnham KJ (2007) The redox chemistry of the Alzheimer's disease amyloid beta peptide. *Biocheim Biophys Acta* 1768: 1976-1990.

Soosairajah J, Maiti S, Wiggan O, Sarmiere P, Moussi N, Sarcevic B, Sampath R, Bamburg JR, Bernard O (2005) Interplay between components of a novel LIM kinase-slingshot phosphatase complex regulates cofilin. *EMBO J* 24:473-486.

Sperling RA, Laviolette PS, O'Keefe K, O'Brien J, Rentz DM, Pihlajamaki M, Marshall G, Hyman BT, Selkoe DJ, Hedden T, Buckner RL, Becker JA, Johnson KA (2009) Amyloid deposition is associated with impaired default network function in older persons without dementia. *Neuron* 63:178-188

Stine WB, Jr., Dahlgren KN, Krafft GA, LaDu MJ (2003) In vitro characterization of conditions for amyloid-beta peptide oligomerization and fibrillogenesis. *J Biol Chem* 278:11612-11622.

Stokin GB, Goldstein LS (2006) Axonal transport and Alzheimer's disease. *Annu Rev Biochem* 75:607-627.

Stoppini L, Buchs PA, Muller D (1991) A simple method for organotypic cultures of nervous tissue. *J Neurosci Methods* 37:173-182.

Sun X, Tong Y, Qing H, Chen CH, Song W (2006a) Increased BACE1 maturation contributes to the pathogenesis of Alzheimer's disease in Down syndrome. *FASEB J* 20:1361-1368.

Sun X, He G, Song W (2006b) BACE2 as a novel APP theta-secretase, is not responsible for the pathogenesis of Alzheimer's disease in Down syndrome. *FASEB J* 20:1369-1376

Tanzi RE, Bertram L (2005) Twenty years of the Alzheimer's disease amyloid hypothesis: a genetic perspective. *Cell* 120:545-555.

Townsend M, Shankar GM, Mehta T, Walsh DM, Selkoe DJ (2006) Effects of secreted oligomers of amyloid beta-protein on hippocampal synaptic plasticity: a potent role for trimers. *J Physiol* 572:477-492.

Velasco ME, Smith MA, Siedlak SL, Nunomura A, Perry G (1998) Striation is the characteristic abnormality in Alzheimer disease. *Brain Res* 813:329-333.

Vincent JL, Snyder AZ, Fox MD, Shannon BJ, Andrews JR, Raichle ME, Buckner RL (2006) Coherent spontaneous activity identifies a hippocampal-parietal memory network. *J Neurophysiol* 96:3517-3531.

Walsh DM, Klyubin I, Fadeeva JV, Cullen WK, Anwyl R, Wolfe MS, Rowan MJ, Selkoe DJ (2002) Naturally secreted oligomers of amyloid beta protein potently inhibit hippocampal long-term potentiation *in vivo*. *Nature* 416:535-539.

Wang HW, Pasternak JF, Kuo H, Ristic H, Lambert MP, Chromy B, Viola KL, Klein WL, Stine WB, Krafft GA, Trommer BL (2002) Soluble oligomers of beta amyloid (1-42) inhibit long-term potentiation but not long-term depression in rat dentate gyrus. *Brain Res* 924:133-140.

Whiteman IT, Gervasio OL, Cullen KM, Guillemin GJ, Jeong EV, Witting PK, Antao ST, Minamide LS, Bamburg JR, Goldsbury C (2009) Activated ADF/cofilin sequesters phosphorylated microtubule associated protein during assembly of Alzheimer-like neuronal cytoskeletal striations *J Neurosci* 29:12994-13005.

Yuen EY, Yan Z (2009) Dopamine D4 receptors regulate AMPA receptor trafficking and glutamatergic transmission in GABAergic interneurons of prefronatl cortex. *J Neurosci* 14:550-562.

Zhao WQ, De Felice FG, Fernandez S, Chen H, Lambert MP, Quon MJ, Krafft GA, Klein WL (2008) Amyloid beta oligomers induce impairment of neuronal insulin receptors. *FASEB J* 22:246-260.